Glatt H, Schneider H, Liu Y. 2005. V79-hCYP2E1-hSULT1A1, a cell line for the sensitive detection of genotoxic effects induced by carbohydrate pyrolysis products and other food-borne chemicals. Mutat Res 580:41–52.

Hakura A, Shimada H, Nakajima M, Sui H, Kitamoto S, Suzuki S, Satoh T. 2005. Salmonella/human S9 mutagenicity test: A collaborative study with 58 compounds. Mutagen 20:217–228.

Hargreaves MB, Jones BC, Smith DA, Gescher A. 1994. Inhibition of *p*-nitrophenol hydroxylase in rat liver microsomes by small aromatic and heterocyclic molecules. Drug Metab Dispos 22: 806–810.

Hashimoto K, Tanii H. 1985. Mutagenicity of acrylamide and its analogues in *Salmonella typhimurium*. Mutat Res 158:129–133.

Honma M, Hayashi M, Sofuni T. 1997. Cytotoxic and mutagenic responses to X-rays and chemical mutagens in normal and p53-mutated human lymphoblastoid cells. Mutat Res 374:89–98.

IARC. Acrylamide. In:IARC Monographs on the Evaluation of Carcinogen Risk to Human: Some Industrial Chemicals, Vol. 60. Lyon: International Agency for Research on Cancer. Lyon. 1994. pp 389–433.

Ikeda T, Nishimura K, Taniguchi T. 2001. In vitro evaliation of drug interaction caused by enzyme inhibition-HAB protocol. Xenobiol Metabol Dispos 16:115–126.

Knaap AG, Kramers PG, Voogd CE, Bergkamp WG, Groot MG, Langebroek PG, Mout HC, van der Stel JJ, Verharen HW. 1988. Mutagenic activity of acrylamide in eukaryotic systems but not in bacteria. Mutagen 3:263–268.

Koyama N, Sakamoto H, Sakuraba M, Koizumi T, Takashima Y, Hayashi M, Matsufuji H, Yamagata K, Masuda S, Kinae N, Honma M. 2006. Genotoxicity of acrylamide and glycidamide in human lymphoblastoid TK6 cells. Mutat Res 603:151–158.

Lahdetie J, Suutari A, Sjoblom T. 1994. The spermatid micronucleus test with the dissection technique detects the germ cell mutagenicity of acrylamide in rat meiotic cells. Mutat Res 309:255–262.

Manjanatha MG, Aidoo A, Shelton SD, Bishop ME, MacDaniel LP, Doerge DR. 2005. Evaluation of mutagenicity in Big Blue (BB) mice administred acrylamide (AA) and glycidamide (GA) in drinking water for 4 weeks. Environ Mol Mutagen 44:214.

Matsushima T, Hayashi M, Matsuoka A, Ishidate M Jr, Miura KF, Shimizu H, Suzuki Y, Morimoto K, Ogura H, Mure K, Koshi K, Sofuni T. 1999. Validation study of the in vitro micronucleus test in a Chinese hamster lung cell line (CHL/IU). Mutagen 14:569–580.

Mei N, Hu J, Churchwell MI, Guo L, Moore MM, Doerge DR, Chen T. 2008. Genotoxic effects of acrylamide and glycidamide in mouse lymphoma cells. Food Chem. Toxicol 46:628–636.

Moore MM, Amtower A, Doerr C, Brock KH, Dearfield KL. 1987. Mutagenicity and clastogenicity of acrylamide in L5178Y mouse lymphoma cells. Environ Mutagen 9:261–267.

Mottram DS, Wedzicha BL, Dodson AT. 2002. Acrylamide is formed in the Maillard reaction. Nature 419:448–449.

Oda Y, Nakamura S, Oki I, Kato T, Shinagawa H. 1985. Evaluation of the new system (umu-test) for the detection of environmental mutagens and carcinogens. Mutat Res 147:219–229.

Oda Y, Aryal P, Terashita T, Gillam EM, Guengerich FP, Shimada T. 2001. Metabolic activation of heterocyclic amines and other procarcinogens in *Salmonella typhimurium* umu tester strains expressing human cytochrome P4501A1, 1A2, 1B1, 2C9, 2D6, 2E1, and 3A4 and human NADPH-P450 reductase and bacterial *O*-acetyltransferase. Mutat Res 492:81–90.

Omori T, Honma M, Hayashi M, Honda Y, Yoshimura I. 2002. A new statistical method for evaluation of L5178Ytk(+/−) mammalian cell mutation data using microwell method. Mutat Res 517:199–208.

Rice JM. 2005. The carcinogenicity of acrylamide. Mutat Res 580:3–20.

Sandhu P, Guo Z, Baba T, Martin MV, Tukey RH, Guengerich FP. 1994. Expression of modified human cytochrome P450 1A2 in *Escherichia coli*: Stabilization, purification, spectral characterization, and catalytic activities of the enzyme. Arch Biochem Biophys 309:168–177.

Segerback D, Calleman CJ, Schroeder JL, Costa LG, Faustman EM. 1995. Formation of *N*-7-(2-carbamoyl-2-hydroxyethyl)guanine in DNA of the mouse and the rat following intraperitoneal administration of [14C]acrylamide. Carcinogenesis 16:1161–1165.

Shelby MD, Cain KT, Cornett CV, Generoso WM. 1987. Acrylamide: Induction of heritable translocation in male mice. Environ Mutagen 9:363–368.

Sofuni T, Hayashi M, Matsuoka A, Sawada M. 1985. Mutagenicity tests on organic chemical concominants in city water and related compounds. II. Chromosome aberration tests in cultured mammalian cells. Eisei Shiken Hok 103:64–75.

Stadler RH, Blank I, Varga N, Robert F, Hau J, Guy PA, Robert MC, Riediker S. 2002. Acrylamide from Maillard reaction products. Nature 419:449–450.

Sumner SC, Fennell TR, Moore TA, Chanas B, Gonzalez F, Ghanayem BI. 1999. Role of cytochrome P450 2E1 in the metabolism of acrylamide and acrylonitrile in mice. Chem Res Toxicol 12:1110–1116.

Sumner SC, Williams CC, Snyder RW, Krol WL, Asgharian B, Fennell TR. 2003. Acrylamide: A comparison of metabolism and hemoglobin adducts in rodents following dermal, intraperitoneal, oral, or inhalation exposure. Toxicol Sci 75:260–270.

Suzuki S, Kurata N, Nishimura Y, Yasuhara H, Satoh T. 2000. Effects of imidazole antimycotics on the liver microsomal cytochrome P450 isoforms in rats: Comparison of in vitro and ex vivo studies. Eur J Drug Metab Pharmacokinet 25:121–126.

Tareke E, Rydberg P, Karlsson P, Eriksson S, Tornqvist M. 2000. Acrylamide: A cooking carcinogen? Chem Res Toxicol 13:517–522.

Tareke E, Rydberg P, Karlsson P, Eriksson S, Tornqvist M. 2002. Analysis of acrylamide, a carcinogen formed in heated foodstuffs. J Agric Food Chem 50:4998–5006.

Tornqvist M. 2005. Acrylamide in food: The discovery and its implications: A historical perspective. Adv Exp Med Biol 561:1–19.

Tsuda H, Shimizu CS, Taketomi MK, Hasegawa MM, Hamada A, Kawata KM, Inui N. 1993. Acrylamide; induction of DNA damage, chromosomal aberrations and cell transformation without gene mutations. Mutagen 8:23–29.

Wu YQ, Yu AR, Tang XY, Zhang J, Cui T. 1993. Determination of acrylamide metabolite, mercapturic acid by high performance liquid chromatography. Biomed Environ Sci 6:273–280.

Xiao Y, Tates AD. 1994. Increased frequencies of micronuclei in early spermatids of rats following exposure of young primary spermatocytes to acrylamide. Mutat Res 309:245–253.

Zeiger E, Anderson B, Haworth S, Lawlor T, Mortelmans K, Speck W. 1987. Salmonella mutagenicity tests. III. Results from the testing of 255 chemicals. Environ Mutagen 9(Suppl 9):1–109.

Accepted by—
K. Dearfield

J. Radiat. Res., 50, 407–413 (2009)

An Approach to Estimate Radioadaptation from DSB Repair Efficiency#

Fumio YATAGAI[1]*, Kaoru SUGASAWA[2], Shuichi ENOMOTO[1] and Masamitsu HONMA[3]

Radioadaptation/I-SceI digestion/DSB repair/TK6 cells.

In this review, we would like to introduce a unique approach for the estimation of radioadaptation. Recently, we proposed a new methodology for evaluating the repair efficiency of DNA double-strand breaks (DSB) using a model system. The model system can trace the fate of a single DSB, which is introduced within intron 4 of the *TK* gene on chromosome 17 in human lymphoblastoid TK6 cells by the expression of restriction enzyme I-SceI. This methodology was first applied to examine whether repair of the DSB (at the I-SceI site) can be influenced by low-dose, low-dose rate gamma-ray irradiation. We found that such low-dose IR exposure could enhance the activity of DSB repair through homologous recombination (HR). HR activity was also enhanced due to the pre-IR irradiation under the established conditions for radioadaptation (50 mGy X-ray–6 h–I-SceI treatment). Therefore, radioadaptation might account for the reduced frequency of homozygous loss of heterozygosity (LOH) events observed in our previous experiment (50 mGy X-ray–6 h–2 Gy X-ray). We suggest that the present evaluation of DSB repair using this I-SceI system, may contribute to our overall understanding of radioadaptation.

INTRODUCTION

It is important to accurately estimate human health risks for persons occupationally exposed to ionizing radiation (IR), such as airline crews and workers in medical and industrial fields. For estimating such risks, it is worthwhile to investigate radioadaptation, that is, acquiring a cellular radioresistance to a challenging IR by a pre-exposure to low-dose IR. Radioadaptation was first reported by Olivieri *et al.*[1] The priming radiation exposure delivered by labeling human lymphocytes with tritiated thymidine caused a decrease in chromosomal aberration frequency after a challenging exposure to 1.5 Gy of IR. That discovery stimulated a series of studies using human lymphocytes and various mammalian cell lines as described in reviews.[2,3] A reduced induction of both micronuclei and sister chromatid exchanges was shown in Chinese hamster V79 cells pre-exposed to low doses of γ-rays or ^{3}H β-rays.[4] Subsequent studies reported similar radioadaptive responses, such as reduced mutation frequencies in human lymphocytes,[5] mouse SR-1 cells[6] and human-hamster hybrid A_L cells,[7] an altered mutation spectrum in human-hamster hybrid A_L cells,[7] reduced micronucleus frequencies in human lymphocytes[8] and mouse embryo cells,[9] and reduced deletions and rearrangements in human lymphoblast cells.[10] Those studies suggest that radioadaptation is an important defense mechanism against a high-dose IR, although the molecular mechanisms involved remain largely unknown.[11–15]

Cellular responses such as a bystander effect, genetic instability, and hyper-radiosensitivity are reported to be tightly related to the radioadaptation.[16–21] In mammalian cells, for example, bystander mutagenesis may be suppressed by an adaptive response.[16] Another example is the possible involvement of a "radioadaptive bystander" effect in human lung fibroblasts.[22] The reduction of radiosensitivity in cells with a wild type *p53* gene by a radiation-induced, nitric oxide (NO)-mediated bystander effect may also be a manifestation of the radioadaptation.[21,23] This possibility is supported by the finding that the NO-induced apoptosis observed in lymphoblastoid and fibroblast cells depends on the phosphorylation and activation of p53.[24] In fact, p53 was suggested to play a key role in the mechanisms of an adaptive response

*Corresponding author: Phone: +81-48-467-9710,
Fax: +81-48-467-9710,
E-mail: yatagai@riken.jp

[1]Metallomics Imaging Research Unit, Center for Molecular Imaging Science, The Institute of Physical and Chemical Research (RIKEN), Saitama 351-0198, Japan; [2]Biosignal Research Center, Kobe University, Hyogo 657-8501, Japan; [3]Division of Genetics and Mutagenesis, National Institute of Health Sciences, Tokyo 158-8501, Japan.

#Translated and modified from Radiat. Biol. Res. Comm. Vol.43(4); 443–453, (2008, in Japanese).
doi:10.1269/jrr.09050

mediated by a feedback signaling pathway involving protein kinase C (PKC), p38 mitogen activated protein kinase (p38MAPK), and phospholipase C (PLC).[11,13,25]

One of the possible targets for radioadaptation is oxidative base damage. A low-dose rate whole body γ-irradiation of mice (1.2 mGy/h, total 0.5 Gy) demonstrated the activation of antioxidative enzymes such as MnSOD and catalase in spleen cells, leading to less DNA damage as determined by a comet assay.[26] Furthermore, down-regulation of the human *CDC16* gene that occurs after oxidative stress causes more rapid and efficient repair in adapted (2 cGy pre-irradiated) human lymphoblastoid cells challenged with 4 Gy irradiation.[12] However, oxidative base excision repair enzymes, including DNA glycosylases, hOGG1, and hNth1, are reportedly not up-regulated at the post-transcriptional level in γ-ray-primed TK6 cells.[27] Those reports suggest that the antioxidant defense machinery is likely to be involved in radioadaptation although the mechanisms involved are still not well understood.

Gene expression also seems to be tightly related to a variety of functions in the adaptive response such as the induction of antioxidant defense machinery, repair of DNA damage, control of cell-cycle progression, *etc.* In fact, *de novo* synthesis of transcripts and proteins is reported to be required for the expression of the adaptive response.[28] Following that report, gene expression analysis has been extensively studied by many investigators.[15,28–31] For example, the *CHD6* gene in human lymphoblastoid cell AHH-1 can be up-regulated by 0.5 Gy of γ-irradiation and its induced expression could be involved in a low-dose hypersensitive response.[29] Recently, gene profiles in the kidney and testis from γ-irradiated (485 days at dose rates of 0.032–13 μGy/min) mice were determined using oligonucleotide microarrays, and differentially expressed genes were identified.[31]

DNA double strand breaks (DSBs) are a most serious type of DNA damage. They can be caused by IR or radiomimetic chemicals, and they can occur spontaneously during DNA replication. The nonrepair or misrepair of DSBs can cause cell death or mutagenic and/or carcinogenic consequences, so the accurate repair of DSBs is important for maintaining genomic integrity.[32,33] In other words, DSB repair is an essential function in all living organisms. Recently analyses using nondividing lymphocyte and fibroblast cells suggested that the adaptive response is not mediated by an enhanced rejoining of DNA strand breaks but rather is a reflection of perturbation in cell cycle progression.[34] On the other hand, the induction of an efficient chromosome repair system by the priming radiation dose is considered to be involved in radioadaptation mechanisms, and in fact, the efficiency of DSB repair in Chinese hamster V79 cells exposed to γ-rays is enhanced by a priming exposure of 5 cGy of γ-rays.[35] The reduced frequencies of chromosomal alterations as described above supports the latter possibility of DSB-repair enhancement. At the present stage, it is difficult to conclude which factor, cell-cycle perturbation or DSB repair, largely contributes to radioadaptation.

THE I-SCEI SYSTEM FOR DSB REPAIR EVALUATION

Outline of the system

A model system was constructed for evaluating DSB repair by tracing the fate of a single DSB on chromosomal DNA. The DSB generated in this system can be considered as a target DNA-lesion susceptible to repair, and this system can distinguish two major DSB repair pathways, non-homologous end-joining (NHEJ) and homologous recombination (HR) (Fig. 1).[36,37] The human lymphoblastoid cell line TSCE5 is heterozygous (+/–) for the thymidine kinase (*TK*) gene and the line TSCER2 is compound heterozygous (–/–; two different TK^- alleles); both carry an I-SceI endonuclease recognition site in intron 4 on one allele of the *TK* gene. DSBs can be generated at the I-SceI site by expression of the I-SceI vector.[36,37] When DSBs occur at the *TK* locus, NHEJ in TSCE5 cells produces TK-deficient mutants while HR between the *TK* alleles in TSCER2 cells produces TK-proficient revertants. This means that positive-negative drug selection for TK phenotypes permits distinction between NHEJ and HR repair.

Cell line construction for use in the system

Details of the strain construction are described in our previous work (Fig. 2).[36] Briefly, in lymphoblastoid TK6 cells heterozygous for the *TK* gene, the functional allele was first inactivated by gene targeting with vector pTK4 to

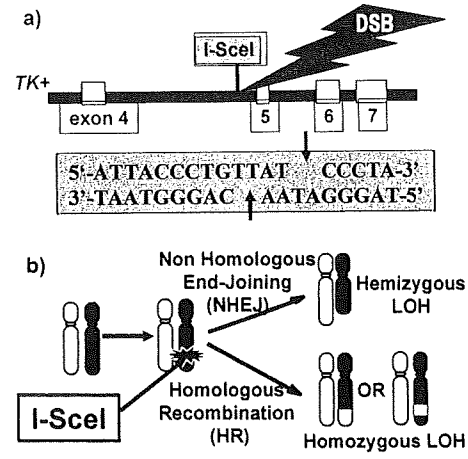

Fig. 1. Principle of DSB formation and repair evaluation. A single DNA double strand break (DSB) is generated at the I-SceI recognition site in a human lymphoblastoid TK6 cell by transfecting an I-SceI expression vector (a) and the efficiencies of DSB repair through non-homologous end-joining (NHEJ) or homologous repair (HR) are evaluated from induction of hemizygous and homozygous LOH events, respectively (see text).

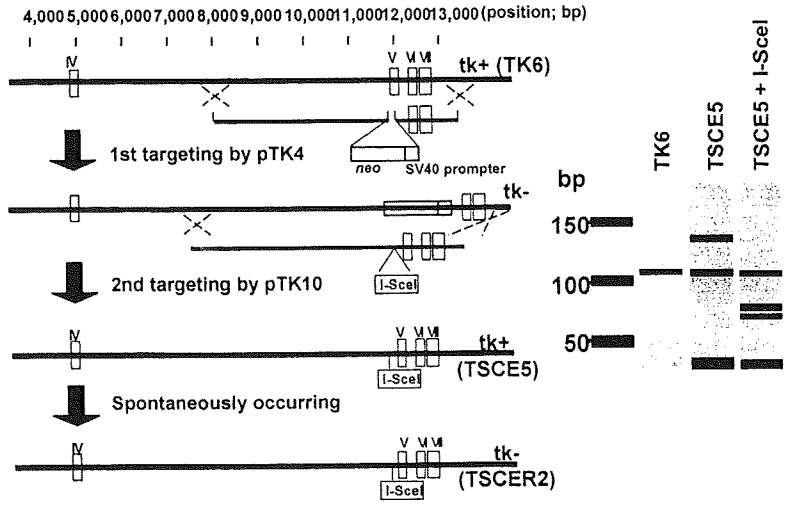

Fig. 2. Cell line construction. In the TK6 cell line, the functional allele of *TK* gene was first inactivated by gene targeting vector pTK4 and then the I-SceI recognition site was introduced at 75 bp upstream of exon 5 in the *TK* gene. The new line was termed TSCE5 and its compound heterozygote (*TK*–/–) cell line, TSCER2, was also isolated (see text).

replace exon 5 of the *TK* gene by a *neo* gene. To introduce the I-SceI recognition site at 75 bp upstream of exon 5, the targeting vector pTK10, encompassing about 6 kb of the original *TK* gene with exons 5, 6, and 7, and the I-SceI recognition site in intron 4, was used to revert the *TK* gene disrupted by pTK4. The new line was termed TSCE5. A spontaneous mutation in a TSCE5 cell (G to A in position 23 of exon 5), which we cloned, led to the compound heterozygote (*TK*–/–) cell line, TSCER2.

I-SceI expression for introduction of DSB

We introduced the I-SceI expression vector (pCBASce) by electroporation methodology using Nucleofector Kit V (amaxa AG, Cologne, Germany) (Fig. 3).[36–38] The I-SceI expression vector was introduced into about 65% of the cells at 24 hr after the transfection and the expression last for 3 days incubation.[37] The relatively long expression allowed us to succeed in estimating the influence of low-dose, low-dose-rate γ-rays irradiation on DSB repair, especially the effect of post-IR-exposure, as described below.

Evaluation of DSB repair efficiencies

Measurements of TK^- mutants and TK^+ revertants allow us to evaluate DSB repair efficiencies through NHEJ and HR pathways, respectively (Fig. 3). In TSCE5, when a DSB at the I-SceI site is repaired by NHEJ involving a deletion in the adjacent exon, the cell can be isolated as a TK-deficient mutant. In TSCER2, when a DSB is repaired by HR between the *TK* alleles, a TK^+ allele can be generated, resulting in a revertant phenotype. The DSB repair *via* NHEJ was 73–86 times higher than that *via* HR in our previous studies.[36,37] These findings are consistent with the report that NHEJ is the major repair pathway in mammalian cells.[39]

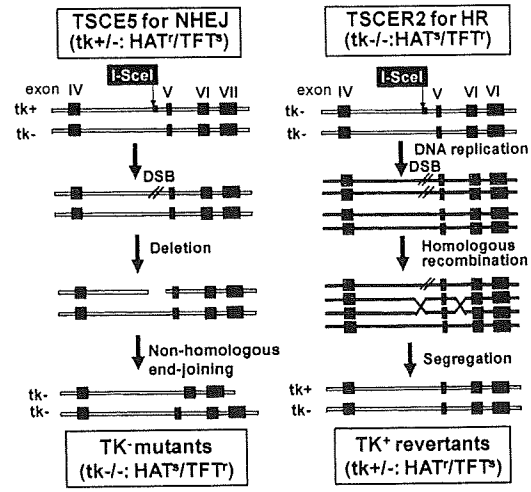

Fig. 3. An approach to evaluate DSB repair efficiency. In TSCE5, when a DSB at the I-SceI site is repaired by NHEJ involving a deletion in the adjacent exon, the cell can be isolated as a TK-deficient mutant. In TSCER2, when a DSB is repaired by HR between the *TK* alleles, a TK^+ allele can be generated, resulting in a revertant phenotype (see text). Filled exons represent TK mutations.

APPLICATION OF THE I-SCEI SYSTEM FOR EVALUATING RADIOADAPTATION IN TERMS OF DSB REPAIR

Influence of low-dose, low-dose-rate γ-rays on DSB repair

The I-SceI digestion system was applied for estimating the influence of low-dose, low-dose-rate γ-irradiation on repair of a site-specifically introduced DSB (Fig. 4).[38] The results

obtained with Mode A (30 mGy of pre-γ-irradiation) and Mode B (8.5 mGy of post-γ-irradiation) are shown in Tables 1 and 2, respectively. The NHEJ repair of DSB was little influenced by either modes of low-dose, low dose-rate γ-irradiation. DSB repair by HR, in contrast, was enhanced by ~50% and ~80% in Mode A and Mode B, respectively. This might implicate that both pre-γ-irradiation (Mode A) and post-γ-irradiation (Mode B) induce a radioadaptation, although both modes of irradiations, especially Mode B, are different from the original concept of radioadaptation. In fact, DSBs are generated during the γ-irradiation in Mode B, because I-SceI expression lasts for 3 days incubation as previously mentioned.

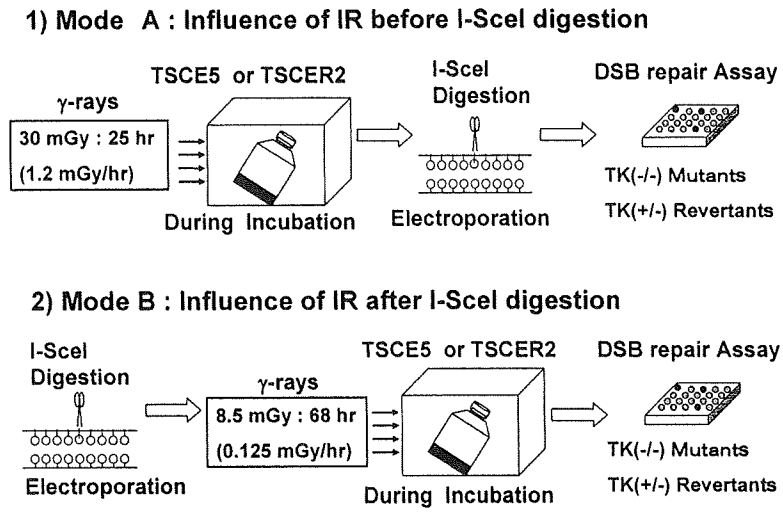

Fig. 4. Influence of low-dose IR exposure on DSB repair. Experimental schemes of radiation exposure and I-SceI expression are illustrated. Mode A: cells were exposed to low-dose, low-dose-rate γ-rays and then transfected with the I-SceI vector by electroporation (see text). 2) Mode B: cells were transfected with the I-SceI vector and then exposed to γ-rays at a much lower dose and dose-rate (see text).

Table 1. Effect of pre-IR exposure on DSB repair (Mode A).

a) NHEJ efficiency in TSCE5 cells

Exp.	Mutant Frequency, MF ($\times 10^{-6}$)				Effect of IR (Relative MF*)
	Control	γ-rays	I-SceI	γ-rays + I-SceI	
1	3.5	6.1	8600	8500	0.99
2	1.8	3.2	2900	3200	1.1
Average	2.7	4.7	5800	5900	1.0 (P = 0.82)

*Relative MF was calculated as MF (γ-rays + I-SceI)/MF (I-SceI).

b) HR efficiency in TSCER2 cells

Exp.	Revertant Frequency, RF ($\times 10^{-6}$)				Effect of IR (Relative RF*)
	Control	γ-rays	I-SceI	γ-rays + I-SceI	
1	–	–	90	114	1.3
2	–	–	62	96	1.5
3	–	–	25	45	1.8
Average	–	–	59	85	1.5 (P = 0.021)

*Relative RF was calculated as RF (γ-rays + I-SceI)/RF (I-SceI).

Table 2. Effect of post-IR exposure on DSB repair (Mode B).

a) NHEJ efficiency in TSCE5 cells

Exp.	Mutant Frequency, MF ($\times 10^{-6}$)				Effect of IR (Relative MF*)
	Control	γ-rays	I-SceI	γ-rays + I-SceI	
1	2.8	1.3	3400	4500	1.3
2	3.1	2.8	12000	17000	1.4
3	–	–	11000	11000	1.0
Average	3.0	2.1	8800	10800	1.2 (P = 0.12)

*Relative MF was calculated as MF (γ-rays + I-SceI)/MF (I-SceI).

b) HR efficiency in TSCER2 cells

Exp.	Revertant Frequency, RF ($\times 10^{-6}$)				Effect of IR (Relative RF*)
	Control	γ-rays	I-SceI	γ-rays + I-SceI	
1	–	–	82	160	2.0
2	–	–	160	270	1.7
3	–	–	110	190	1.7
Average	–	–	120	210	1.8 (P = 0.0013)

*Relative RF was calculated as RF (γ-rays + I-SceI)/RF (I-SceI).

Influence of low-dose X-ray irradiation on DSB repair

We have extensively studied the effects of low-dose IR by using a loss of heterozygosity (LOH) analysis system.[40–42] The thymidine kinase deficient (TK^-) mutants induced in TK6 cells can be classified as LOH type and non-LOH type by this system. The LOH mutants were further classified as homozygous-type and hemizygous-type, and the replaced or deleted part of the chromosome was identified by so-called chromosome mapping. In addition to this kind of analysis at the chromosome level, non-LOH mutants were further characterized at the DNA sequence level to confirm that the mutation occurs in the *TK* gene or not. Recently we could establish the optimum condition for mutagenic radioadaptation in TK6 cells.[43] Under such condition as shown in Fig. 5, the greatest reduction in *TK* mutation frequency was observed in TK6 cells exposed to a challenging X-ray irradiation (2 Gy), and the TK^- mutants so obtained were analyzed by the LOH system.[43]

The TK^- mutation frequency (MF) obtained after the challenging X-ray (2 Gy) exposure, 18.3×10^{-6} was reduced to 11.4×10^{-6} (62% of the original level) by inducing the radioadaptation (50 mGy of pre-X-irradiation at 6 hr before the above challenging X-irradiation; Fig. 6). LOH analysis could classify the TK^- mutational events as non-LOH (mostly mutations in the *TK* gene), hemizygous LOH (deletion of chromosome) and homozygous LOH (homologous recombination [HR] between chromosomes), as mentioned above.[40–42] Non-LOH events are, in theory, classified as chromosomal alterations, but most of non-LOH mutants obtained in this experiment were confirmed to be small mutations in the *TK* gene by DNA base sequencing of mRNA obtained from the mutants.[43] The pre-irradiation decreased the frequencies of non-LOH events and homozygous LOH events to 27% and 60% of the original levels, respectively. The frequency of hemizygous LOH events, however, was not significantly altered by the pre-irradiation. Since LOH events are most likely the consequence of DSB repair, we tried to investigate the influence of priming X-ray irradiation on DSB repair efficiency under the optimum condition for radioadaptation.

The repair efficiency of DSB *via* NHEJ was hardly influenced by the pre-irradiation of 50 mGy X-rays (Table 3). On the other hand, a ~70% enhancement in HR repair of DSB was observed after this treatment. The enhanced activity of HR observed in this experiment could reflect the activity of error-free DSB repair, providing a reduction in genetic alterations at the chromosome level. In fact, we observed a ~60% reduction in the induction of homozygous LOH as mentioned above. The chromosome-mapping analysis demon-

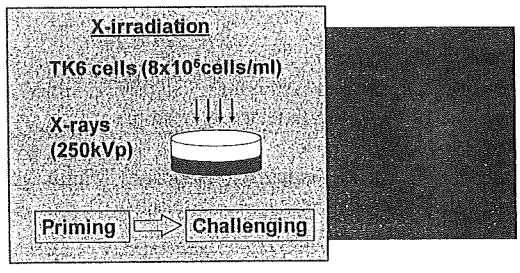

Fig. 5. An experimental scheme for mutagenic radioadaptation. The optimum conditions providing the greatest reduction in the frequency of *TK* mutations induced after a challenging X-ray (2 Gy) irradiation of TK6 cells, are shown in the right panel of this figure. The details have already been described in our previous work.[43]

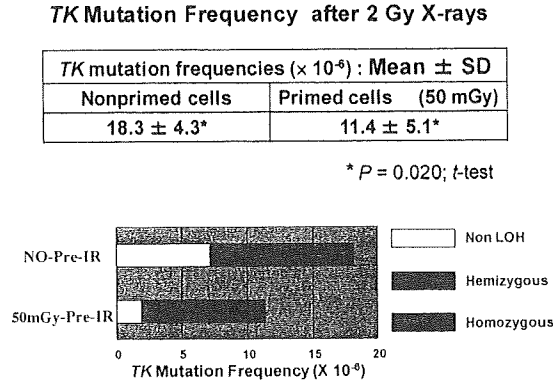

Fig. 6. Genetic analysis of radioadaptation induced by low-dose X-rays. Results of the *TK* mutation assay performed under the optimum condition for radioadaptation (Fig. 5) are summarized in the table, and the classification of the isolated TK^- mutants was made by LOH analysis and the results are shown in the histograms (see text).

Table 3. The effect of a priming X-ray exposure on DSB repair (X-ray - X-ray adaptive experiment).

a) NHEJ efficiency in TSCE5 cells

Exp.	Effect of IR (Relative MF*)
1	0.98
2	0.76
3	0.99
Average	0.91

*Relative MF was calculated as MF (X-rays + I-SceI)/MF (I-SceI).

b) HR efficiency in TSCER2 cells

Exp.	Effect of IR (Relative RF*)
1	2.2
2	1.2
3	1.7
Average	1.7

*Relative RF was calculated as RF (X-rays + I-SceI)/RF (I-SceI).

strated that the observed homozygous LOH events were mostly of the crossing-over type.[23] In contrast, the analysis of TK (+/–) revertants observed with our DSB repair assay suggests that HR in this I-SceI system mostly reflects a gene conversion activity, with a relatively small proportion of non-crossing-over events (data not shown). More supporting evidence is required to determine if an enhanced HR activity is reflected by the reduction in homozygous LOH events.

Further applications and perspectives

It is of theoretical and practical importance to estimate human health risks from low-doses of ionizing radiation. One example is the risk for astronauts exposed to space radiation, because the background radiation in space is, at least, more than 100-fold higher than the background level found on earth. Currently, we have the opportunity to study the influence of space radiation in TK6 cells, which were recently brought back to earth after preservation for more than four months, mostly in a frozen state, in the International Space Station. Assuming that the DNA damage caused by space radiation has been accumulated in the frozen cells, such damage could induce mutations when the cells begin to grow again. Furthermore, such damage might have the potential ability to induce radioadaptation and this radioadaptation might be detected as an enhancement in DSB repair in the I-SceI digestion system in the recovered cells.

The following points involved in our I-SceI digestion system merit discussion. Because our I-SceI system does not uncover all NHEJ and HR events, it is difficult to evaluate accurately the extent of DSB repair *via* both HR and NHEJ pathways. For example, our system does not monitor sister-chromatid HR, which is probably the major HR pathway in mammalian cells. Small gene conversion events, which do not extend into the exon 5 region, can also not be detected by this system. Although the I-SceI system may over-estimate the repair efficiency of NHEJ compared with HR, this methodology can still be considered to contribute to elucidating the DSB repair associated with low-dose IR exposure.

Finally, we would like to emphasize that the present evaluation of DSB repair using the I-SceI system, may contribute to our overall understanding of radioadaptation. Other types of studies regarding gene expression, epigenetic changes *etc.*, are also required for a more complete understanding.

ACKNOWLEDGMENTS

The authors greatly appreciate Professor Takeo Ohnishi of Nara Prefecture Medical University for providing us with the opportunity to present our work. They also appreciate Dr. Alasdair Gordon of Baylor College of Medicine in USA for preparing the manuscript of the present paper. This study was supported by the Budget for Nuclear Research of the Ministry of Education, Culture, Sports, Science and Technology, and was reviewed by the Atomic Energy Commission of Japan.

REFERENCES

1. Olivieri, G., Bodycote, Y. and Wolf. S. (1984) Adaptive response of human lymphocytes to low concentrations of radioactive thymidine. Science **223**: 594–597.
2. Wolf, S. (1996) Aspects of the adaptive response to very low doses of radiation and other agents. Mutat. Res. **358**: 135–142.
3. Wolf, S. (1998) The adaptive response in radiobiology: Evolving insights and implications. Environ. Health Perspect. **106**: 277–283.
4. Ikushima, T. (1987) Chromosomal response to ionizing radiation reminiscent of an adaptive response in cultured Chinese hamster cells. Mutat. Res. **180**: 215–221.
5. Sanderson, B. J. S. and Morely, A. A. (1986) Exposure of human lymphocytes to ionizing radiation reduces mutagenicity by subsequent radiation. Mutat. Res. **164**: 347–151.
6. Zhou, P. K., Liu, X. Y., Sun, W. Z., Zhang, Y. P. and Wei, K. (1993) Cultured mouse SR-1 cells exposed to low-dose of γ-rays become less susceptible to the induction of mutations by radiation as well as bleomycin. Mutagenesis **8**: 109–111.
7. Ueno, A. M., Vannais, D. B., Gustafson, S. L., Wong, J. C. and Waldren, C. A. (1996) A low adaptive dose of gamma-rays reduced the number and altered the spectrum of S1 mutants in human hamster hybrid cells. Mutat. Res. **358**: 161–169.
8. Wojewodska, M., Kruzewski, M., Iwanenko, K. and Szumiel, I. (1997) Effects of signal transduction in adapted lymphocytes: micronuclei frequency and DNA repair. Int. J. Radiat. Biol. **71**: 245–252.
9. Azzam, E. I., Raaphorst, G. P. and Mitchel, R. E. (1994) Radiation-induced adaptive response for protection against micronucleus formation and neoplastic transformation in C3H 10T1/2 mouse embryo cells. Radiat. Res. **138**: S28–S31.
10. Rigaud, O., Papadopoulo, D. and Moustacchi, E. (1993) Decreased deletion mutation in radioadapted human lymphoblast. Radiat. Res. **133**: 94–101.
11. Rigaud, O. and Moustacchi, E. (1996) Radioadaptation for gene mutation and the possible molecular mechanisms of the adaptive response. Mutat. Res. **358**: 127–134.
12. Zhou, P.-K. and Rigaud, O. (2001) Down-regulation of the human *CDC16* gene after exposure to ionizing radiation: A possible role in the radioadaptive response. Radiat. Res. **155**: 43–49.
13. Sasaki, M. S., Ejima, Y., Tachibana, A., Yamada, T., Ishizaki, K., Shimizu, T. and Nomura, T. (2002) DNA damage response pathway in radioadaptive response. Mutat. Res. **504**: 101–118.
14. Szumiel, I. (2005) Adaptive responses: Stimulated DNA repair or decreased damage fixation? Int. J. Radiat. Biol. **81**: 233–241.
15. Coleman, M. A., Yin, E., Peterson, L. E., Nelson, D., Sorensen, K., Tucker, J. D. and Wyrobeck, A. J. (2005) Low-dose irradiation alters the transcript profiles of human lymphoblastoid cells inducing genes associated with radioadaptive response. Radiat. Res. **164**: 369–382.
16. Swant, S. G., Randers-Pehrson, G., Metting, N. F. and Hall,

E. J. (2001) Adaptive response and the bystander effect induced by radiation in C3H 10T1/2 cells in culture. Radiat. Res. **156**: 177–180.
17. Zhou, H. N., Randers-Pehrson, G., Geard, C. R., Brenner, D. J., Hall, E. J. and Hei, T. K. (2003) Interaction between radiation-induced adaptive response and bystander mutagenesis in mammalian cells. Radiat. Res. **160**: 512–516.
18. Bonner, W. M. (2003) Thresholds, bystander effect, and adaptive response. Proc. Natl. Acad. Sci. USA, **100**: 4973–4975.
19. Mitchell, S. A., Marino, S. A., Brenner, D. J. and Hall, E. J. (2004) Bystander effect and adaptive response in C3H 10T (1/2) cells. Int. J. Radiat. Biol. **80**: 465–472.
20. Hei, T. K., Persaud, R., Zhou, H. and Suzuki, M. (2004) Genotoxicity in the eyes of bystander cells. Mutat. Res. **568**: 111–120.
21. Matsumoto, H., Hamada, N., Takahashi, A., Kobayashi, Y. and Ohnishi, T. (2007) Vanguards of paradigm shift in radiation biology: radiation-induced adaptive and bystander responses. J. Radiat. Res. **48**: 97–106.
22. Iyer, R. and Lehnert, B. E. (2002) Low-dose, low-LET ionizing radiation-induced radioadaptation and associated early responses in unirradiated cells. Mutation Res. **503**: 1–9.
23. Matsumoto, H., Takahashi, A. and Ohnishi, T. (2004) Radiation-induced adaptive and bystander effects. Biol. Sci. Space **18**: 247–254.
24. McLaughlin, L. M. and Demple, B. (2005) Nitric oxide-induced apoptosis in lymphoblastoid and fibroblast cells dependent on the phosphorylation and activation of p53. Cancer Res. **65**: 6097–6104.
25. Shimizu, T., Kato, T. Jr., Tachibana, A. and Sasaki, M. S. (1999) Coordinated regulation of radioadaptive response by protein kinase C and p38 nitrogen-activated protein kinase. Exp. Cell. Res., **251**: 424–432.
26. Otsuka, K., Koana, T., Tauchi, H. and Sakai, K. (2006) Activation of antioxidative enzymes induced by low-dose-rate whole body γ irradiation: adaptive response in terms of initial DNA damage. Radiat. Res. **166**: 474–478.
27. Inoue, M., Shen, G-P., Chaudhry, M. A., Galick, H., Blaisdell, J. O. and Wallace, S. S. (2004) Expression of the oxidative base excision repair enzymes is not induced in TK6 human lymphoblastoid cells after low doses of ionizing radiation. Radiat. Res. **161**: 409–417.
28. Yongblom, J. H., Wiencke, J. K. and Wolf, S. (1989) Inhibition of the adaptive response of human lymphocytes to very low doses of ionizing radiation by the protein synthesis inhibitor cycloheximide. Mutat. Res. **227**: 257–261.
29. Wang, H. P., Long, X. H., Sun, Z. Z., Rigaud, O., Xu, Q. Z., Huang, Y. C., Sui, J. L., Bai, B. and Zhou, P. K. (2006) Identification of differentially transcribed genes in human lymphoblastoid cells irradiated with 0.5 Gy of γ-ray and the involvement of low dose radiation inducible CHD6 gene in cell proliferation and radiosensitivity. Int. J. Radiat. Biol. **82**: 181–190.
30. Ding, L.-H., Shingyoji, M., Chen, F., Hwang, J.-J., Burma, S., Lee, C., Chen, J.-F. and Chen, D. J. (2005) Gene expression profiles of normal human fibroblasts after exposure to ionizing radiation: a comparative study of low and high doses. Radiat. Res. **164**: 17–26.
31. Taki, K., Wang, B., Nakajima, T., Wu, J., Ono, T., Uehara, Y., Matsumoto, T., Oghiso, Y., Tanaka, K., Ichinohe, K., Nakamura, S., Tanaka, S., Magae, J., Kakimoto, A. and Nenoi, M. (2009) Microarray analysis of differentially expressed genes in the kidneys and testes of mice after long-term irradiation with low-dose-rate γ-rays. J. Radiat. Res. **50**: 241–252.
32. Jackson, S. P. (2002) Sensing and repairing DNA double-strand breaks. Carcinogenesis **23**: 687–696.
33. Valerie, K. and Povirk, L. F. (2003) Regulation and mechanisms of mammalian double-strand break repair. Oncogene **22**: 5792–5812.
34. Cramers, P., Atanasova, P., Vrolijk, H., Darroudi, F., van Zeeland, A. A., Huiskamp, R., Mullenders, L. H. F., Kleinjans and Jos, C. S. (2005) Pre-exposure to low-doses: modulation of X-ray-induced DNA damage and repair? Radiat. Res. **164**: 383–390.
35. Ikushima, T., Aritomi, H. and Morisita, J. (1996) Radioadaptive response: efficient repair of radiation- induced DNA damage in adapted cells. Mutat. Res. **358**: 193–198.
36. Honma, M., Izumi, M., Sakuraba, M., Tadokoro, S., Sakamoto, H. Wang, W., Yatagai, F. and Hayashi, M. (2003) Deletion, rearrangement, and gene conversion; genetic consequences of chromosomal double-strand breaks in human cells. Environ. Mol. Mutagen **42**: 288–298.
37. Honma, M., Sakuraba, M., Koizumi, T., Takashima, T., Sakamoto, H. and Hayashi, M. (2007) Non-homologous end-joining for repairing I-SceI induced DNA double strand breaks in human cells. DNA Repair **6**: 781–788.
38. Yatagai, F., Suzuki, M., Ishioka, N., Ohmori, H. and Honma. M. (2008) Repair of I-SceI Induced DSB at a specific site of chromosome in human cells: influence of low-dose, low-dose rate gamma-rays. Radiat. Environ. Biophys. **47**: 439–444.
39. Pastwa, E. and Blasiak, J. (2003) Non-homologous end-joining. Acta Biochem. Pol. **50**: 891–908.
40. Morimoto, S., Kato, T., Honma, M., Hayashi, M., Hanaoka, F. and Yatagai, F. (2002) Detection of genetic alterations induced by low-dose X rays: analysis of loss of heterozygosity for *TK* mutation in human lymphoblastoid cells. Radiat. Res. **157**: 533–538.
41. Morimoto, S., Honma, M. and Yatagai, F. (2002) Sensitive detection of LOH events in a human cell line after C-ion beam exposure. J. Radiat. Res. **43** (Suppl.): S163–S167.
42. Umebayashi, Y., Honma, M., Abe, T., Ryuto, H., Suzuki, H., Shimazu, T., Ishioka, N., Iwaki, M. and Yatagai, F. (2005) Mutation induction after low-dose carbon-ion beam irradiation of frozen human cultured cells. Biol. Sci. Space **19**: 237–241.
43. Yatagai, F., Umebayashi, Y., Honma, M., Sugasawa, K., Takayama, Y. and Hanaoka, F. (2008) Mutagenic radioadaptation in a human lymphoblastoid cell line. Mutat. Res. **638**: 48–55.

Received on April 27, 2009
Revision received on July 1, 2009
Accepted on July 13, 2009
J-STAGE Advance Publication Date: August 13, 2009

Pathology International 2009; **59**: 161–166 doi:10.1111/j.1440-1827.2009.02344.x

Original Article

Establishment of novel mAb to human ERC/mesothelin useful for study and diagnosis of ERC/mesothelin-expressing cancers

Kiyoshi Ishikawa,[1] Tatsuya Segawa,[1] Yoshiaki Hagiwara,[1,2] Masahiro Maeda,[1] Masaaki Abe[2] and Okio Hino[2]

[1]*Immuno-bioligical Laboratories, Takasakishi, Gunma and* [2]*Department of Pathology and Oncology, Juntendo University School of Medicine, Hongo, Tokyo, Japan*

Malignant mesothelioma is a highly aggressive tumor of the serosal cavity that arises from the mesothelial cells of the pleura, peritoneum, or pericardium. The immunohistochemical diagnosis of epithelioid mesothelioma from biopsy or surgically resected specimens has been actively pursued, using markers such as mesothelin. Several markers have indeed been helpful for confirming the diagnosis of mesothelioma and distinguishing between mesothelioma and adenocarcinoma. The authors have developed a novel mAb to human C-ERC/mesothelin, which performed well when used in western blotting, fluorescence-activated cell sorting, immunocytochemistry and immunohistochemistry, and which therefore will be useful in studying the molecular biology of mesothelin, in addition to improving the diagnosis and therapy of mesothelin-expressing cancers.

Key words: diagnosis, ERC/mesothelin, malignant mesothelioma, monoclonal antibody

Mesothelioma is an aggressive tumor arising from the serosal surface, such as the pleural and peritoneum, and it has a dismal prognosis.[1] Several recent studies have described the safe utilization of aggressive multimodality therapy and have found evidence for the effectiveness of combination chemotherapy regimens using pemetrexed and cisplatin.[2–4] The prognosis after this type of therapy, however, remains poor.

A study by Sugarbaker *et al.* reporting a 5 year survival of 40% for selected patients following trimodality therapy, demonstrated that early diagnosis is vital to improve the prognosis.[2] In light of the difficulty, however, of making an early diagnosis of mesothelioma using current diagnostic imaging techniques, the identification of tumor markers for mesothelioma is needed urgently.[5–7] While no reliable serum marker for mesothelioma has yet been found, Robinson *et al.* have recently proposed a soluble mesothelin-related protein as a candidate.[1]

Previously, we discovered the renal carcinoma gene *ERC*, which we found was expressed highly in renal cancers in the Eker rat.[8] Furthermore, we subsequently confirmed that the *ERC* gene is a homolog of the human mesothelin gene, a gene expressed strongly in normal mesothelial cells, mesothelioma, non-mucinous ovarian carcinomas and pancreatic ductal adenocarcinomas.[9,10] The human mesothelin gene codes for several proteins. Its primary product is a 71 kDa precursor protein, which is cleaved physiologically by a furin-like protease into a 40 kDa *C*-terminal fragment, C-ERC/mesothelin, which remains membrane-bound, and a 31 kDa *N*-terminal fragment, N-ERC/mesothelin, which is secreted into the blood.[11] The resultant *C*-terminal 40 kDa fragment is classified as a mesothelin, and its presence in the serum has been reported as a useful tumor marker in mesothelioma patients.[12] In contrast, the *N*-terminal 31 kDa fragment, which is a secreted protein and has been cloned as a megakaryocyte-potentiation factor, has been reported as a useful tumor marker for mesothelioma or any other cancer.[6]

In the present study we report on the establishment of a novel mAb for human C-ERC/mesothelin. This antibody should be useful in studying the molecular biology of mesothelin, and also improve the diagnosis of and therapy for mesothelin-expressing cancers.

MATERIALS AND METHODS

Human subjects

Our study for the tumor marker of mesothelioma was approved by the Institutional Review Broad of Juntendo

Correspondence: Okio Hino, MD, PhD, Department of Pathology and Oncology, Juntendo University School of Medicine, 2-1-1 Hongo, Tokyo 113-8421, Japan. Email: ohino@juntendo.ac.jp

Received 25 July 2008. Accepted for publication 3 November 2008.

University School of Medicine, its hospital, and Immuno-Biological Laboratories. Patients gave their signed informed consent.

Cell lines

The mesothelioma cell lines, NCI-H226 and MESO-4 were obtained from Dr Usami.[13] These were maintained in TIL media supplemented with 10% fetal bovine serum.

Generation of a human C-ERC/mesothelin-GST fusion protein by *Escherichia coli*

The human *C-ERC/mesothelin* cDNA was cloned from the total RNA of the human cervical carcinoma cell line HeLaS3 using polymerase chain reaction. Primers used were as follows: forward, 5′-GGAGTGGAGAAGACAGCCTGT-3′; reverse, 5′-GCCCTGTAGCCCCAGCCC-3′. cDNA for human *C-ERC/mesothelin* was inserted between the EcoRI and XhoI into pGEX-6P (GE-Healthcare Bio-sciences, Piscataway, NJ, USA). The C-ERC/mesothelin-GST fusion protein was directed into the periplasm of *E. coli.* The fusion protein was purified with Glutathione Sepharose 4B Beads (GE-Healthcare Bio-sciences). The purified proteins were quantified using Protein assay kit (Pierce, Rockford, IL, USA) and checked on sodium dodecylsulfate (SDS)-PAGE. The purity of the bacterial C-ERC/mesothelin was >95%.

Immunization and cell fusion

Female mice (6–8 weeks old; BALB/c, Charles River, Japan) were immunized four to six times weekly with human C-ERC/mesothelin-GST fusion protein (50 μg/mouse) and one boost was given with the fusion proteins i.p. before fusion. The spleen was harvested 84–90 h after the last boost and fused with X63-Ag8.653 myeloma cells.

Screening with enzyme immunoassay on human C-ERC/mesothelin-GST fusion protein

Screening for hybridomas was performed with an enzyme immunoassay (EIA). Nunc Immuno plates (Nalge Nunc International, Rochester, NY, USA) were coated with the fusion protein (50 ng/well in 0.1 mol/L carbonate buffer, pH 9.5) and incubated overnight at 4°C. Plates were then blocked with blocking buffer (PBS with 1% bovine serum albumin (BSA) and 0.05% sodium azide) overnight at 4°C and washed with a washing buffer (PBS with 0.05% Tween20). The plates were incubated with the hybridoma supernatant for 1 h at 37°C. After washing with the washing buffer, the plates were incubated with a peroxidase-conjugated goat anti-mouse IgG antibody in washing buffer. Finally, the plates were washed again with the washing buffer and hydrogen peroxide/o-phenylenediamine was added to each well. The color was allowed to develop for 15 min at room temperature and the reaction was stopped by the addition of a stop solution (1 N sulfuric acid). The plates were read at 490 nm using an automated plate reader (Molecular Device, Sunnyvale, CA, USA). The selected hybridomas were grown in a Celline flask (Integra Bioscience, Chur, Switzerland). The cell culture supernatant was affinity-purified with affinity column chromatography using Protein A column (GE-Healthcare Bio-sciences).

Epitope mapping of the anti-human C-ERC/mesothelin mouse mAb

For the determination of the epitope of the anti-human C-ERC/mesothelin mouse mAb, we produced the C-ERC/mesothelin-GST fusion protein in four different molecular sizes by cutting a human *C-ERC/mesothelin* gene into four 200 bp fragments. The fusion proteins were analyzed on western blot for epitope mapping.

Western blot

Cell lysates of the human mesothelioma cell line or C-ERC/mesothelin-GST fusion protein for epitope mapping were separated on 12.5% SDS-PAGE under reducing conditions. Proteins were transferred to a PVDF membrane (Millipore, Billerica, MA, USA). After blocking with a blocking solution (PBS with 3% non-fat dried milk, 1% BSA and 0.05% Tween20), the membrane was incubated with 1 μg/mL of each mAb overnight at 4°C, followed by a peroxidase-conjugated goat anti-mouse IgG antibody. Proteins were visualized with an ECL detection system (GE-Healthcare Bio-sciences).

Fluorescence-activated cell sorting

Cultured cells (2×10^5) were dissociated with dissociation buffer. Each sample was washed twice in fluorescence-activated cell sorter (FACS) buffer (PBS with 5% BSA, 0.1% sodium azide). An anti-human C-ERC/mesothelin mouse mAb was added to the cells and incubated for 30 min at 4°C. Cells were then washed with FACS buffer, and incubated with 2 μg/mL Alexa 488 goat anti-mouse IgG (Molecular Probe, Eugene, OR, USA) for 30 min at 4°C. Finally, cells

were washed with FACS buffer and analyzed on a FACScan system (Becton Dickinson, Franklin Lakes, NJ, USA).

Immunocytochemistry

Cultured cells or cells derived from the ascites were smeared on coverslips and air-dried for 30 min. Coverslips were fixed with cold acetone for 10 min at room temperature followed by 1% paraformaldehyde for 5 min at 4°C. Non-specific binding sites were blocked by incubating with 5% normal goat serum in PBS for 15 min at room temperature. The coverslips were incubated with the primary antibodies (2 μg/mL) for 1 h at room temperature. After washing with PBS, the coverslips were incubated with Envision+ (DakoCytomation, Kyoto, Japan), followed by detection of peroxidase with diaminobenzidine-peroxide substrate solution. The sections were counterstained with hematoxylin.

Immunohistochemistry

Formaldehyde-fixed paraffin-embedded tissue sections from patients with mesothelioma were evaluated for C-ERC/mesothelin expression. The sections were deparaffinized in xylene, followed by graded ethanol hydration into water. The sections were heated in Target Retrieval Solution, 10 mmol/L citrate buffer (pH 6.0) (DakoCytomation), for antigen retrieval. The sections were then incubated with the primary antibodies (1 μg/mL) overnight at 4°C. After washing with the washing buffer, the sections were incubated with Envision (DakoCytomation), followed by detection of peroxidase with diaminobenzidine-peroxide substrate solution. The sections were counterstained with hematoxylin.

RESULTS

Generation of recombinant human C-ERC/mesothelin-GST fusion protein with *E. coli* and establishment of new mAb for human C-ERC/mesothelin

To establish new mAb for human C-ERC/mesothelin, we generated a human C-ERC/mesothelin-GST fusion protein using *E. coli*. The fusion proteins were used for immunization and screening for the hybridoma supernatant with an EIA. Finally, eight clones were identified that reacted selectively with the fusion protein coated to plates. The specificity of the anti-human C-ERC/mesothelin mAb was determined immunohistochemically with the section from mesothelioma patients, the results of which showed that one clone from among the eight clones, 22A31, had a high affinity for human C-ERC/mesothelin. In these studies, we compared them with a commercially available mAb, 5B2 (Novocastra, Newcastle, UK), and found them to be useful in western blotting, FACS, immunocytochemistry and immunohistochemistry for human C-ERC/mesothelin.

Epitope mapping of clone 22A31, the anti-human C-ERC/mesothelin mAb

To determine the epitope of the anti-human C-ERC/mesothelin mAb, clone 22A31, we prepared four different molecular sizes of the C-ERC/mesothelin-GST fusion protein by cutting a human C-ERC/mesothelin gene into four 200 bp fragments. The fusion proteins were analyzed on western blot for epitope mapping. As a result (Fig. 1), we confirmed that the epitope 22A31 was on the *N*-terminal portion of C-ERC/mesothelin.

Western blot

The expression of human C-ERC/mesothelin in mesothelioma cell lines was analyzed on western blot (Fig. 2). This antibody detected one major product in the lysate of the

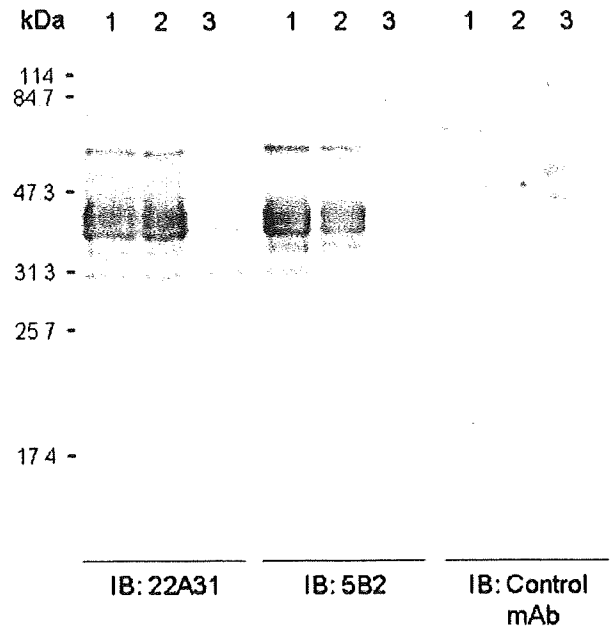

Figure 2 Western blot analysis of the clone 22A31. This antibody (1 μg/mL) detected one major product in the cell lysates of human mesothelioma cell lines, NCI-H226 (lane 1) and MESO-4 (lane 2). Control mAb did not react to the mesothelioma cell lines. Lane 3, control ERC/mesothelin-negative cell line.

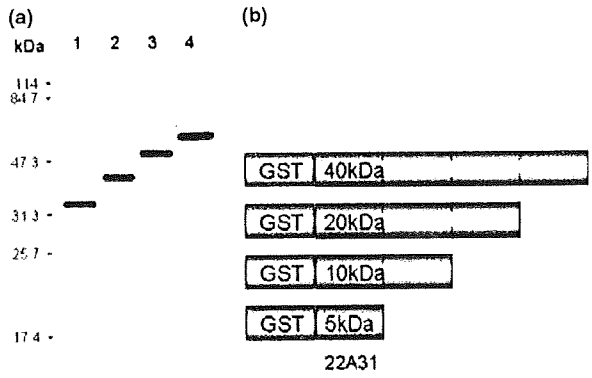

Figure 1 Epitope mapping of the clone 22A31. The epitope was on the *N*-terminal portion of C-ERC/mesothelin. (**a**) Western blot analysis for epitope mapping of (**b**) C-ERC/mesothelin-GST fusion protein in four different molecular sizes, which were produced by cutting a human C-ERC/mesothelin gene into four 200 bp fragments. The clone 22A31 reacted against every fragment. This indicates that the epitope of 22A31 was on the *N*-terminal portion of C-ERC/Mesothelin. Lane 1, GST-C-ERC/mesothelin (5 kDa); lane 2, GST-C-ERC/mesothelin (10 kDa); lane 3, GST-C-ERC/mesothelin (20 kDa); lane 4, GST-C-ERC/mesothelin (40 kDa).

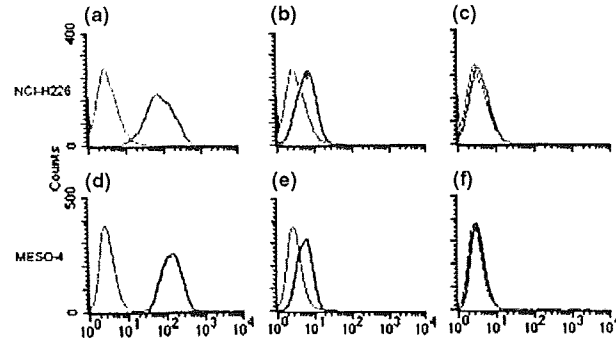

Figure 3 Fluorescence-activated cell sorting of the (**a**,**d**) clone 22A31. This antibody (2 μg/mL) bound to NCI-H226 and MESO-4. (**c**,**f**) Control mAb did not react to the mesothelioma cell lines. (**b**,**e**) 5B2.

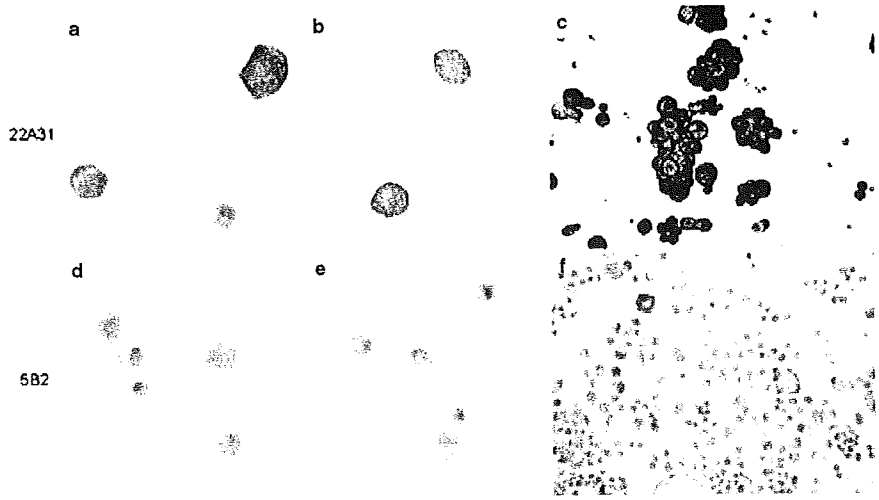

Figure 4 Immunocytochemistry of the clone 22A31. Positive staining was observed in the membranes of human mesothelioma cell lines (**a**) NCI-H226, (**b**) MESO-4 and (**c**) pleural effusion smears obtained from a mesothelioma patient. (**d**–**f**) No staining was seen with 5B2. The coverslips were incubated with the primary antibodies (2 μg/mL).

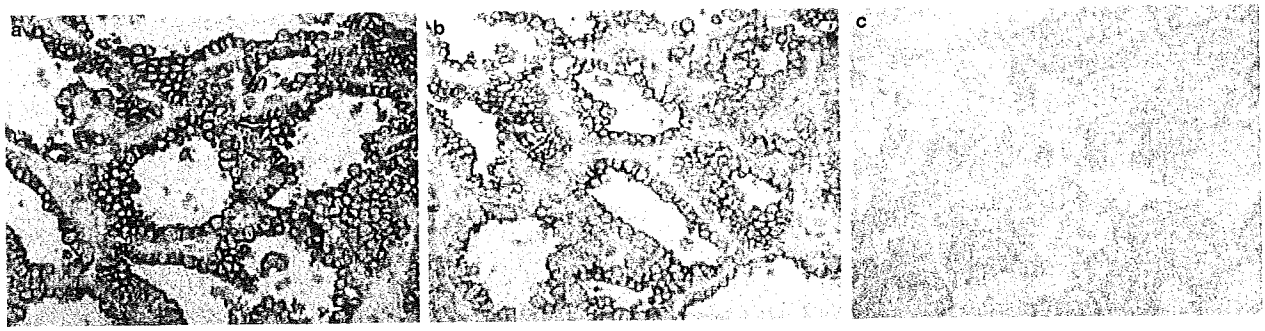

Figure 5 Immunohistochemistry of (**a**) clone 22A31. This antibody (1 μg/mL) strongly reacted to the mesothelioma cell membranes and reacted in a pattern that was comparable to (**b**) 5B2 (1:50 dilution). (**c**) Control mAb did not react to the specimens from malignant mesothelioma patients.

human mesothelioma cell lines, the molecular mass of which was approximately 40 kDa, similar to that of C-ERC/mesothelin. Control mAb did not react to mesothelioma cell lines.

Fluorescence-activated cell sorting

The clone 22A31 was tested on FACS for its ability to bind to the human mesothelioma cell lines. This antibody bound to the human mesothelioma cell lines but did not bind to the ERC/mesothelin-negative cell lines (data not shown). The data in Fig. 3 show that the clone 22A31 generated a large increase in fluorescence intensity compared with the cells incubated with the 5B2 anti-mesothelin mAb. Control mAb did not react to mesothelioma cell lines.

Immunocytochemistry

Immunocytochemical detection of C-ERC/mesothelin in smears of human mesothelioma cell lines, NCI-H226 and MESO-4, is shown in Fig. 4. Strongly positive staining was observed in membranes of these cells, which were reacted with the clone 22A31 (Fig. 4a,b). No staining was seen when the cells were incubated with the 5B2 anti-mesothelin mAb (Fig. 4d,e). The expression of C-ERC/mesothelin in pleural effusion smears obtained from malignant mesothelioma is shown in Fig. 4(c). Membranous expression was observed highly in the smears. The immunocytochemical signal was negative on smears when the 5B2 anti-mesothelin mAb was used (Fig. 4f).

Immunohistochemistry

Immunohistolocalization of ERC/mesothelin in specimens from malignant mesothelioma patients using the anti-human C-ERC/mesothelin mouse mAb is shown in Fig. 5. This antibody reacted to the mesothelioma cell membranes with a pattern that was comparable to the 5B2 anti-mesothelin mAb. This suggests that our newly established antibody could be useful in the immunohistochemical diagnosis of mesothelioma. Control mAb did not react to the specimens from malignant mesothelioma patients.

DISCUSSION

Immunohistochemical diagnosis of epithelioid mesothelioma in pleural biopsy or surgically resected specimens has been actively pursued, using markers such as podoplanin, calretinin, WT-1, cytokeratin 5, thrombomodulin, and mesothelin. Some of these markers used singly and in combination have indeed been helpful for confirming the diagnosis of mesothelioma and distinguishing between mesothelioma and adenocarcinoma, which is one of the challenging problems for the surgical pathologist. In immunohistochemistry for mesothelin, the 5B2 anti-mesothelin mAb is commonly used. In the present study, however, 5B2 had weak or negative reactivity on human mesothelioma cell lines and pleural effusion smears obtained from malignant mesothelioma patients in both FACS and immunocytochemistry. Our newly established mAb 22A31 performed well when used for western blotting, FACS, immunocytochemistry and immunohistochemistry, and could thus be useful in the detection of C-ERC/mesothelin proteins for all types of immunological assay.

The detection of ERC/mesothelin expression on immunohistochemistry and/or immunocytochemistry is important clinically to diagnose patients who are eligible for any therapeutic strategy targeting mesothelin. In addition, the detection and quantification of serum ERC/mesothelin would be helpful for the diagnosis and follow up of patients with mesothelioma, and other mesothelin-expressing cancers.

In conclusion, we have established a new mAb for human C-ERC/mesothelin that performed well in all types of immunological assay. This antibody should be useful in studying the molecular biology of mesothelin, and could also improve the diagnosis of and therapy for mesothelin-expressing cancers.

REFERENCES

1 Robinson BW, Musk AW, Lake RA. Malignant mesothelioma. *Lancet* 2005; **366**: 397–408.
2 Sugarbaker DJ, Flores RM, Jaklitsch MT *et al.* Resection margins, extrapleural nodal status, and cell type of malignant pleural mesothelioma: Results in 183 patients. *J Thorac Cardiovasc Surg* 1999; **117**: 54–63.
3 Vogelzang NJ, Rusthoven JJ, Symanowski J *et al.* Phase III study of pemetrexed in combination with cisplatin versus cisplatin alone in patients with malignant mesothelioma. *J Clin Oncol* 2003; **21**: 2636–44.
4 Sugarbaker DJ, Jaklitsch MT, Bureno R *et al.* Prevention, early detection, and management of complications after 328 consecutive extrapleural pneumonectomies. *J Thorac Cardiovasc Surg* 2004; **128**: 138–46.
5 Maeda M, Hino O. Molecular tumor markers for asbestos-related mesothelioma: Serum diagnosis markers. *Pathol Int* 2006; **56**: 649–54.
6 Shiomi K, Miyamoto H, Segawa T *et al.* A novel ELISA system for detection of a N-ERC/Mesothelin in the sera of mesothelioma patients. *Cancer Sci* 2006; **97**: 928–32.
7 Hino O, Shiomi K, Maeda M. Diagnostic biomarkers of asbestos-related mesothelioma: Example of translational research. *Cancer Sci* 2007; **98**: 1147–51.
8 Hino O, Kobayashi E, Nishizawa M *et al.* Renal carcinogenesis in the Eker rat. *J Cancer Res Clin Oncol* 1995; **121**: 602–5.

9 Yamashita Y, Yokoyama M, Kobayashi E, Takai S, Hino O. Mapping and determination of the cDNA sequence of the Erc gene preferentially expressed in renal cell carcinoma in the Tsc2 gene mutant (Eker) rat model. *Biochem Biophys Res Commun* 2000; **275**: 134–40.
10 Hino O. Multistep renal carcinogenesis in the Eker (Tsc 2 gene mutant) rat model. *Curr Mol Med* 2004; **4**: 807–11.
11 Hassan R, Bera T, Pastan I. Mesothelin: a new target for immunotherapy. *Clin Cancer Ras* 2004; **10**: 3937–42.
12 Hassan R, Remaley AT, Sampson ML *et al.* Detection and quantification of serum mesothelin, a tumor marker for patients with mesothelioma and ovarian cancer. *Clin Cancer Res* 2006; **12**: 447–53.
13 Usami N, Fukui T, Kondo M *et al.* Establishment and characterization of four malignant pleural mesothelioma cell lines from Japanese patients. *Cancer Sci* 2006; **97**: 387–94.

Biochemical and Biophysical Research Communications 390 (2009) 636–641

Contents lists available at ScienceDirect

Biochemical and Biophysical Research Communications

journal homepage: www.elsevier.com/locate/ybbrc

An animal model of preclinical diagnosis of pancreatic ductal adenocarcinomas

Katsumi Fukamachi [a], Hajime Tanaka [b], Yoshiaki Hagiwara [d,e], Hirotaka Ohara [b], Takashi Joh [b], Masaaki Iigo [a], David B. Alexander [a], Jiegou Xu [a], Ne Long [a], Misato Takigahira [f,g], Kazuyoshi Yanagihara [f,h], Okio Hino [e], Izumu Saito [i], Hiroyuki Tsuda [a,c,*]

[a] Department of Molecular Toxicology, Nagoya City University Graduate School of Medical Sciences, 1 Kawasumi, Mizuho-cho, Mizuho-ku, Nagoya 467-8601, Japan
[b] Department of Gastroenterology and Metabolism, Nagoya City University Graduate School of Medical Sciences, 1 Kawasumi, Mizuho-cho, Mizuho-ku, Nagoya 467-8601, Japan
[c] Nanotoxicology Project, Nagoya City University Graduate School of Medical Sciences, 1 Kawasumi, Mizuho-cho, Mizuho-ku, Nagoya 467-8601, Japan
[d] Immuno-Biological Laboratories, 5-1 Aramachi, Takasaki-Shi, Gunma 370-0831, Japan
[e] Department of Pathology and Oncology, Juntendo University School of Medicine, 2-1-1 Hongo, Tokyo 113-8421, Japan
[f] Central Animal Laboratory, National Cancer Center Research Institute, 5-1-1 Tsukiji, Chuo-ku, Tokyo 104-0045, Japan
[g] Gastrointestinal Section, National Cancer Center Hospital, 5-1-1 Tsukiji, Chuo-ku, Tokyo 104-0045, Japan
[h] Laboratory of Health Sciences, Department of Life Sciences, Yasuda Women's University, 6-13-1 Yasuhigashi, Asaminami-ku, Hiroshima 731-0153, Japan
[i] Laboratory of Molecular Genetics, Institute of Medical Science, University of Tokyo, 4-6-1 Shirokanedai, Minato-ku, Tokyo 108-8639, Japan

ARTICLE INFO

Article history:
Received 3 October 2009
Available online 8 October 2009

Keywords:
Pancreas cancer
Serum marker
Erc
Mesothelin
Animal model

ABSTRACT

Pancreatic ductal adenocarcinoma (PDA) is a highly lethal disease, which is usually diagnosed in an advanced stage. Animal PDA models which reflect the human condition are clearly necessary to develop early diagnostic tools and explore new therapeutic approaches. We have established transgenic rats carrying a mutated H- or K-*ras* gene (Hras250 and Kras327) controlled by Cre/loxP activation. These animals develop PDA which are histopathologically similar to that in humans. We utilized this model to identify biomarkers to detect early PDA. We report here that serum levels of Erc/Mesothelin are significantly higher in rats bearing PDA than in controls. Importantly, the levels are significantly elevated in rats before grossly visible carcinomas develop. Even in rats with very small microscopic ductal carcinoma lesions, elevated serum Erc/Mesothelin can be detected. We believe this is the first report of a pancreas tumor animal model in which pre-symptomatic lesions can be diagnosed.

Introduction

Pancreatic ductal adenocarcinoma (PDA) carries the most dismal prognosis of all solid tumors. Preclinical detection of PDA is a necessary first step toward more successful treatment of this disease. Late manifestation of clinical symptoms, as well as the rapid and aggressive course of the disease contribute to its extremely high mortality. Most patients die within 1 year of diagnosis [1], and the 5 year survival rate is <5% [2]. Since the pancreas is located in a retroperitoneal cavity, detection of the tumor mass is possible only when it has reached a relatively large size. Furthermore, markers for the diagnosis of PDA have not yet been established. Consequently, diagnosis of pancreatic cancers when they are still treatable is extremely rare [3].

We have established transgenic rat lines carrying a human $Hras^{G12V}$ (Hras250) [4] or a human $Kras^{G12V}$ (Kras327) oncogene in which the expression of the transgene is regulated by the Cre/loxP system (termed *ras* Tg rats). Targeted activation of the transgene is accomplished by injection of a Cre recombinase-carrying adenovirus (AxCANCre) into the pancreatic ducts through the common bile duct. Neoplastic lesions in the *ras* Tg rats exhibit morphological similarities to those observed in human pancreas lesions. Early ductal lesions exhibit close similarity to intraepithelial neoplasias (PanIN category).

The rat *Erc* (expressed in renal cell carcinoma) gene was identified as a highly expressed gene in renal cell carcinoma of the Eker rat [5,6]. A human homolog of rat *Erc* is the *Mesothelin/megakaryocyte potentiating factor* (*MPF*) gene [7,8]. Mesothelin was identified as a cell surface antigen recognized by the monoclonal antibody K1 in human mesotheliomas and ovarian carcinomas [9–11]; MPF was independently identified in the culture supernatant of a human pancreatic carcinoma cell line, HPC-Y5 [12]. Human Mesothelin/MPF is derived from a common 71 kDa precursor [8,11]. The precursor protein is cleaved by a furin-like protease, and a 31 kDa NH_2-terminal peptide (MPF) is released into the extracellular

Abbreviations: PanIN, pancreatic intraepithelial neoplasias; PDA, pancreas ductal adenocarcinoma; AxCANCre, Cre recombinase-carrying adenovirus; TEF-1, transcription enhancer factor-1

* Corresponding author. Address: Nanotoxicology Project, Nagoya City University Graduate School of Medical Sciences, 1 Kawasumi, Mizuho-cho, Mizuho-ku, Nagoya 467-8601, Japan. Fax: +81 52 853 8996.
E-mail address: htsuda@med.nagoya-cu.ac.jp (H. Tsuda).

0006-291X/$ - see front matter © 2009 Elsevier Inc. All rights reserved.
doi:10.1016/j.bbrc.2009.10.019

space, leaving a 40 kDa COOH-terminal peptide (Mesothelin) attached to the cell surface by a GPI-anchor [9]. To avoid confusion, we refer to the rat Erc protein and its human homolog as Erc/Mesothelin. Erc/Mesothelin is expressed in ovary and pancreas carcinoma tissue in humans [13–15] and can be used as a marker for PDA [15]. Recently, we developed a novel sandwich ELISA system for serum Erc/Mesothelin [16–19]. Using this serum assay system, the level of Erc/Mesothelin was found to be higher in samples from mesothelioma patients than in samples from subjects without pancreas lesions [16,17]. In the present study we report the use of Erc/Mesothelin as a reliable serum marker for pre-symptomatic, pre-malignant pancreas lesions in *ras* Tg rats.

Materials and methods

Animals. Male H*ras*^{G12V} transgenic (Hras250) rats were bred with female Sprague–Dawley rats by CLEA Japan Inc. (Tokyo, Japan) as previously reported [4]. Routine genotyping of Hras250 rats was performed using the primers 5′-TCGTGCTTTACGGTATCGCCGCTCCC GATT-3′ and 5′-GATCTGCTCCCTGTACTGGTGG-3′. For the generation of transgenic rats conditionally expressing human K*ras*^{G12V}, 3× hemagglutinin (HA) tagged K*ras*^{G12V} cDNA was subcloned into the SacI/KpnI site of pCALNL5 (DNA Bank, RIKEN BioResource Center, Ibaraki, Japan). The purified cassette was injected into the pronuclei of Sprague–Dawley rats (CLEA Japan, Tokyo, Japan) as previously reported [4,20]. Two lines were established (Kras301 and Kras327). In this study, we used the Kras327 line. Routine genotyping of Kras327 rats was performed using the primers 5′-TCTGGATCAAATCCGAAC GC-3′ and 5′-TGACCTGCTGTGTCGAGAAT-3′. Rats were maintained in plastic cages in an air-conditioned room with a 12-h light/12-h dark cycle. The experiments were conducted according to the 'Guidelines for Animal Experiments of the Nagoya City University Graduate School of Medical Sciences'.

Tumor induction and pathological examination. AxCANCre was amplified in HEK293 cells and then purified using Vivapure Adenopack (Vivascience, Hannover, Germany). The titer of the adenovirus

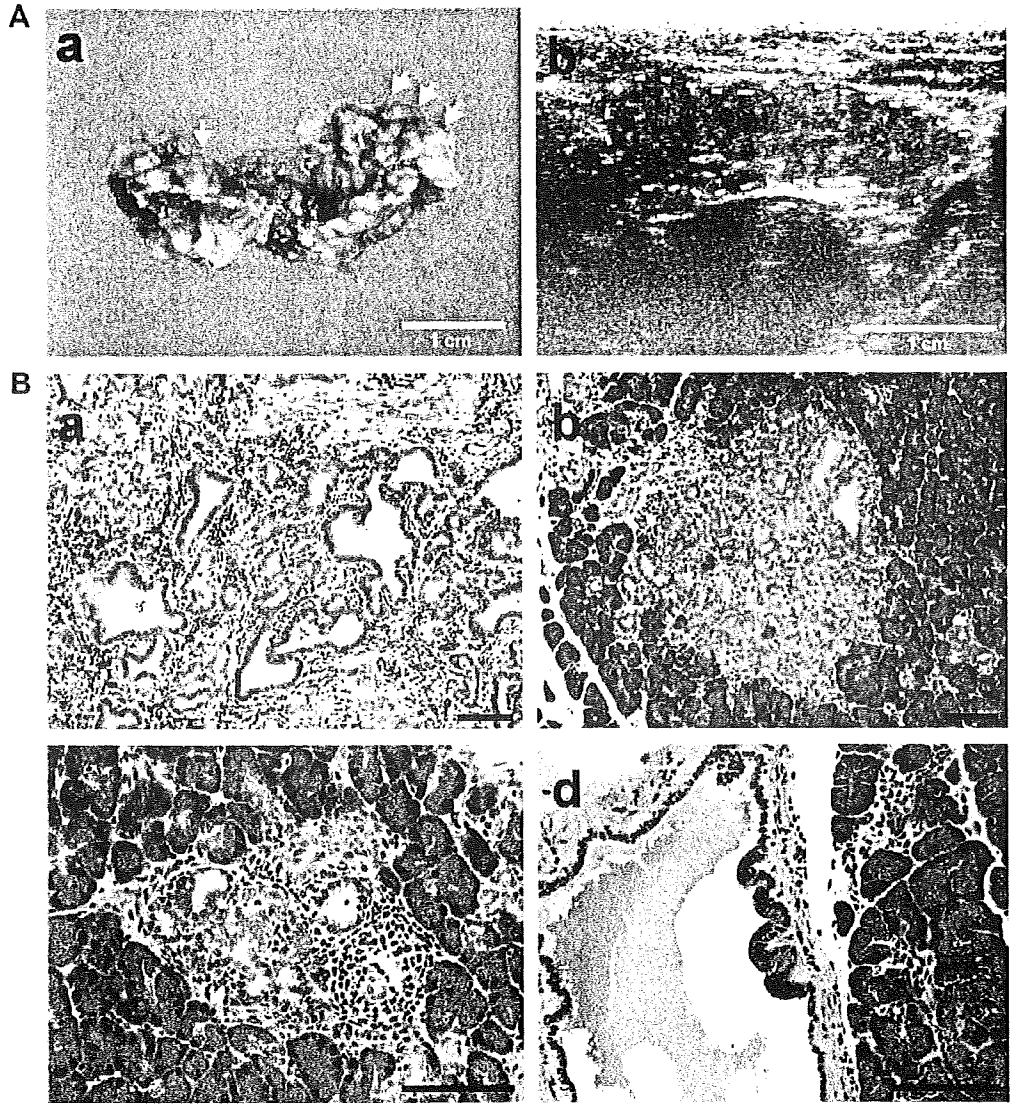

Fig. 1. Pancreas tumors developed in *ras* Tg rats. Animals were killed 3–4 weeks after injection of recombinant AxCANCre into the pancreas of adult *ras* Tg rats. (A) Macroscopic appearance of the pancreas with advanced multiple tumors (arrows) in an Hras250 rat (a). At this stage, multiple tumor nodules can be visualized by ultrasound image analysis (inside broken line) (b). (B) Histological appearance of pancreatic lesions. Large carcinoma (a), small carcinomas (b,c) and a PanIN-1a like lesion with slightly atypical duct epithelium (d). (a,b) are in Hras250 rats and (c) and (d) are grossly invisible small lesions in Kras327 rats. Bars = 100 μm.

Table 1
Microarray data: list of up-regulated genes encoding secreted proteins.

Gene	Accessions	Description	Expression level (tumor/control)
Mmp7	NM_012864	Matrix metalloproteinase-7	18.2
Tf	NM_001013110	Transferrin	14.4
Ctgf	NM_022266	Connective tissue growth factor	14.3
Cx3cl1	NM_134455	Chemokine (C-X3-C motif) ligand 1	7.7
Msln	NM_031658	Erc/Mesothelin	7.4
Lcn2	NM_130741	Lipocalin 2	7.0
Mmp2	U65656	Gelatinase A	6.0
Col18a1	XM_241632	Procollagen, type XVIII, alpha 1	5.5
Mgp	NM_012862	Matrix Gla protein	5.2
Sdc1	NM_013026	Syndecan 1	4.8

was determined using a rapid titer kit (Clontech, Mountain View, CA). Pancreas tumors were induced as described previously [4]. Ultrasound images were acquired using a microimaging system (EUB-8500, Hitachi Medical Corp., Tokyo, Japan). The pancreas was frozen in liquid nitrogen for RNA assays, or fixed in phosphate-buffered 10% formalin and processed for histological observation. Primary antibody anti-rat-C-ERC/Mesothelin (306) (IBL, Gunma, Japan) was used, and staining was performed using Vectastain ABC kits (Vector Laboratories, Burlingame, CA).

Tumors other than PDA were induced by chemical carcinogens, diethylnitrosamine (DEN) for liver cell tumor, *N*-butyl-*N*-(4-hydroxybutyl)nitrosamine (BBN) for bladder tumor, 7,12-dimethylbenz[a]anthracene (DMBA) for mammary tumor, *N*-bis(2-hydroxypropyl)nitrosamine (DHPN) for lung, kidney and thyroid tumor, and DMBA–12-*O*-tetradecanoylphorbol 13-acetate (TPA) for skin tumor.

Establishment of a rat pancreas cell line and Erc/Mesothelin analysis. A pancreas carcinoma cell line was established from a pancreas tumor from an Hras250 rat. The pancreas tumor tissue was placed in RPMI1640 medium at 4 °C. The tumor was diced into 1–2 mm^3 pieces and transplanted to NOD-SCID mice. Three months after transplantation, the tumor grew and reached a size of 10 mm in diameter. Tumor tissues were trimmed of fat and necrotic portions and minced with scalpels. The tissue pieces were transferred to 60-

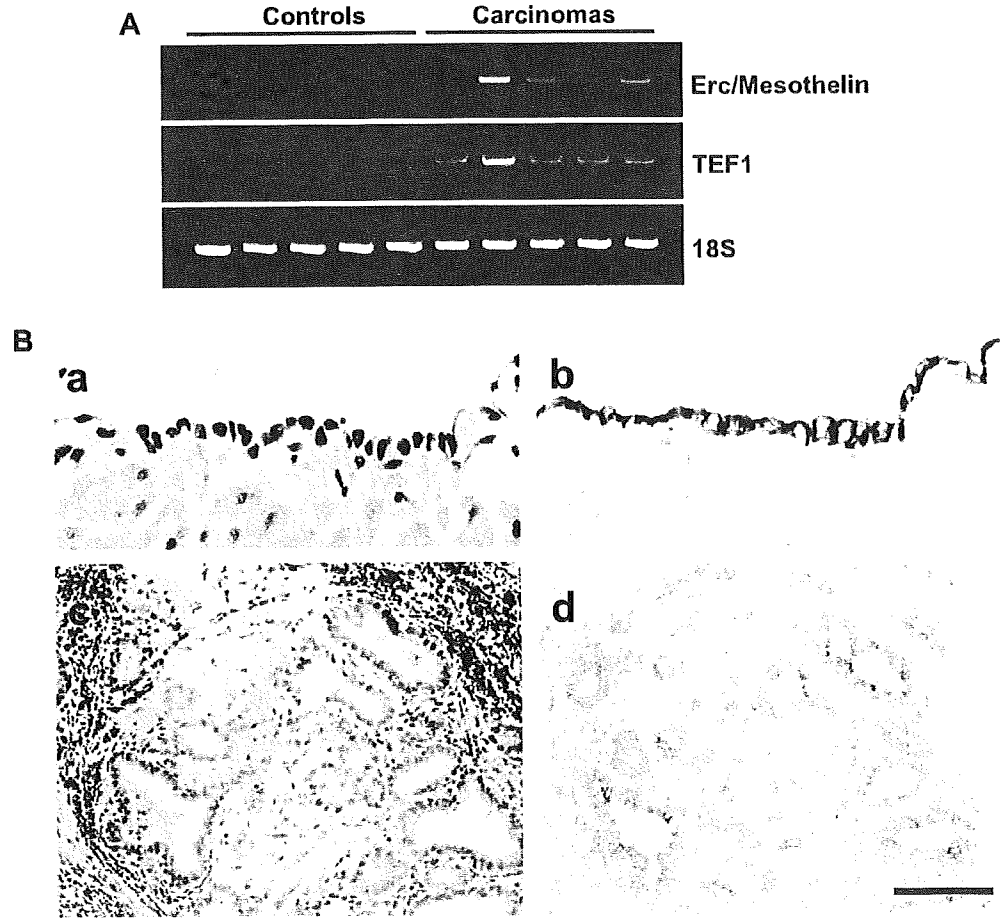

Fig. 2. Expression of Erc/Mesothelin in pancreatic lesions. (A) RT-PCR for Erc/Mesothelin and TEF-1 of normal pancreas and carcinomas in Hras250 rats. Each lane represent RNA prepared from an individual rat. 18S ribosome serves as an RNA control. (B) Immunostaining of Erc/Mesothelin in the mesothelium (a,b) and PDA (c,d) lesions. The antibody is more dense in the apical border. (a,c), H&E staining; (b,d), Erc/Mesothelin staining. Bar = 100 μm.

mm culture dishes at 10–15 fragments/dish. Fibroblasts were removed mechanically and by trypsinization (trypsin, 0.05%; EDTA, 0.02%). The cells were cultured on dishes. The established cell line was maintained in DMEM/Keratinocyte-SFM (Gibco, Grand Island, NY) containing 10% FCS. The cells were seeded in 1 ml of medium at a cell density of 10^5 cells/35-mm plate and cultured for 2 days. Cells were harvested and the cultured supernatant collected.

The tumor cells (1×10^6 or 1×10^7) were transplanted subcutaneously into 6 week old male NOD-SCID mice (Charles River Laboratories Japan, Inc., Yokohama, Japan). After 5 weeks of transplantation, the tumor was weighed and serum was collected for analysis of Erc/Mesothelin.

RT-PCR. Total RNA was isolated using ISOGEN (Nippon Gene, Toyama, Japan). A total of 450 ng of total RNA (from control pancreas and tumor samples) was reverse-transcribed using Superscript III Reverse Transcriptase with Random primers (Invitrogen, Carlsbad, CA). Reverse-transcription reaction mixtures were diluted 1:100 and 2 μl was used for PCR. The following primers were used: *Erc/Mesothelin*, 5′-ACCGTTGACTTTGCCAGTCT-3′ and 5′-TGCATCCGTCTCAC TCACTT-3′; *TEF-1*, 5′-ATTCTTACAGCGACCCGTTG-3′ and 5′-TGCTCCA TGCTCACTATTCG-3′; ribosome 18S, 5′-GTTGGTGGAGCGATTTGTCT-3′ and 5′-GGCCTCACTAAACCATCCAA-3′.

Serum test. The serum level of Erc/Mesothelin was quantified by the ELISA system (Code No.27765, Rat N-ERC/Mesothelin Assay Kit, IBL, Gunma, Japan) described previously [19]. Serum levels of CA19-9, Dupan-2, and SPan-1 were assayed by SRL, Inc. (Tokyo, Japan).

Microarray analysis. For gene microarray analysis, mRNA was isolated from total RNA (pooled sample from five animals) using a "Poly(A)+ Isolation Kit from total RNA" (Nippon Gene) according to the manufacturer's instructions. Microarray analysis was performed by Hokkaido System Science Co., Ltd. (Sapporo, Japan) using Whole Rat Oligo Microarray (Agilent Technologies, Inc., Santa Clara, CA). The experiments were performed twice by switching dyes reciprocally.

Results

Ras Tg rats, 10–30 weeks of age, were killed 3–4 weeks after injection of recombinant AxCANCre into the pancreatic duct via the common bile duct. Many grossly visible whitish tumor nodules were observed throughout the pancreas in both types of *ras* Tg rats, although they were slightly fewer in number in the Kras327 lines. Pancreas tumors developed in all *ras* Tg rats without any relationship to their age. These multiple tumors can be detected by ultrasound imaging (Fig. 1A). Histological examination showed that these nodules were adenocarcinomas with a variable amount of fibrotic tissue proliferation, some showing desmoplastic morphology. Neoplastic lesions were not found in any other organs. Carcinomas caused destruction of pancreas tissue by infiltrative growth, however, remote metastasis was not observed. Representative cases of an advanced carcinoma, early small carcinomas, and a PanIN-1a lesion are shown in Fig. 1B. These pancreas lesions were positive for alucian blue, cytokeratins 19 and 7, cyclooxigenase-2 (COX-2), matrix metalloproteinase-7 (MMP-7), epidermal growth factor (EGF) and EGFR, but negative for amylase, as reported previously [4].

Serum CA19-9, Dupan-2, and SPan-1, which are currently available serum markers for human pancreas cancer, were not detected in pancreas tumor-bearing rats using human antibodies. We performed a comprehensive and global analysis of over 40,000 genes to find diagnosis markers to detect rat PDA. Pancreas tumor tissue with frank ductal adenocarcinomas from Hras250 rats was subjected to microarray analysis. Table 1 lists the top 10 up-regulated genes encoding secreted proteins; secreted proteins are of particular interest for their potential diagnostic value. Our microarray analysis indicated that Erc/Mesothelin was overexpressed 7.4-fold in pancreas carcinoma tissue compared to pancreata of wild type littermates. Importantly, a previous report showed that overexpression of Erc/Mesothelin was identified in the majority of pancreas carcinomas in humans [15]. Therefore, we focused on the preferential expression of Erc/Mesothelin in PDA of *ras* Tg rats.

The expression level of the Erc/Mesothelin gene was confirmed by RT-PCR. Erc/Mesothelin gene expression in pancreatic carcinoma was higher than in the pancreata of wild type littermates (Fig. 2A). Recently, Hucl et al. reported that the presence of transcription enhancer factor (TEF)-1 was required for high cancer-specific expression of Erc/Mesothelin [21]. Similarly, we found that the mRNA expression level of TEF-1 was higher in pancreatic carcinomas than in pancreas tissue from wild type littermates (Fig. 2A). Finally, immunohistochemical studies showed higher expression of Erc/Mesothelin in small carcinoma lesions as compared to surrounding normal tissue (Fig. 2B).

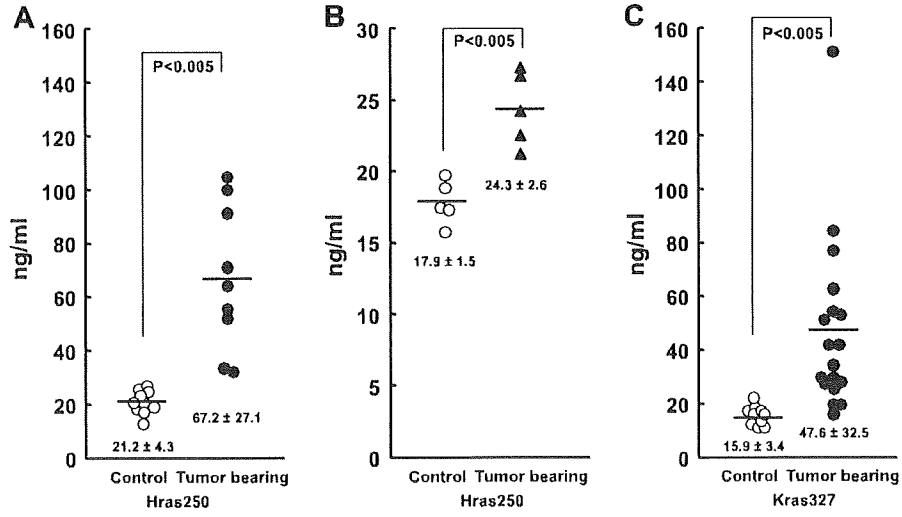

Fig. 3. Levels of N-ERC in rats bearing neoplastic lesions. (A) The serum levels of N-ERC in Hras250 rats bearing multiple pancreas ductal carcinomas was significantly higher than in untreated wild type control littermates ($P < 0.005$). (B) Serum N-ERC in Hras250 rats with early small carcinomas was also significantly higher than in untreated wild type control littermates ($P < 0.005$). The early lesions, not visible by eye, were detected microscopically. (C) The serum level of N-ERC in Kras327 rats bearing multiple pancreas ductal carcinomas was significantly higher than in untreated Kras327 control rats ($P < 0.005$). All animals were sacrificed 3 weeks after the AxCANCre injection.

We initially assayed the serum levels of the NH_2-terminal secretory form of Erc/Mesothelin (N-ERC) in Hras250 rats with pancreas carcinomas and in wild type littermates without pancreas carcinomas (Fig. 3). N-ERC levels in Hras250 rats bearing pancreas carcinomas was 67.2 ± 27.1 ng/ml (mean ± SD) (n = 9), whereas the levels in wild type Hras250 littermates was 21.2 ± 4.3 ng/ml (n = 10) (Fig. 3A). These results confirmed our ability to detect differences in serum N-ERC levels in animals in which Erc/Mesothelin was expressed at high (pancreas tumor-bearing Hras250 rats) and low (wild type littermates without pancreas tumors) levels.

To determine whether elevated levels of N-ERC can be detected in rats with early stage lesions, serum N-ERC levels in Hras250 rats with grossly normal-looking pancreas containing microscopic ductal adenoma/adenocarcinoma lesions were compared to untreated wild type littermates. The levels of N-ERC in rats with early lesions was 24.3 ± 2.6 ng/ml (n = 5) whereas the level in their untreated littermates was 17.9 ± 1.5 ng/ml (n = 5) (P < 0.005) (Fig. 3B). We then measured the levels of N-ERC in untreated Hras250 rats and in Hras250 rats treated with control adenovirus vector. The serum levels of N-ERC were the same in untreated Hras250 rats and Hras250 rats treated with control vector, and these levels were the same or somewhat lower than the levels in the Hras250 wild type littermates (data not shown). These results indicate that in the Hras250 animal model, increased N-ERC can be detected in the serum of animals with pre-malignant lesions.

Next we assayed N-ERC levels in the Kras transgenic rats. The level of N-ERC in tumor-bearing Kras327 rats was 47.6 ± 32.5 ng/ml (n = 18) whereas those of untreated Kras327 rats was 15.9 ± 3.4 ng/ml (n = 10) (P < 0.005) (Fig. 3C). In all serum samples, the COOH-terminal form of Erc/Mesothelin (C-ERC) was undetectable.

Since PDA lesions frequently include variable amounts of mesenchymal tissue, an increase in tumor associated mesothelial cells could cause an increase in serum N-ERC levels. We therefore evaluated the levels in a pancreas carcinoma cell line (designated 634NOD) derived from a pancreas ductal adenocarcinoma from an Hras250 rat. 634NOD cells were implanted subcutaneously into the flank of NOD-SCID mice, and the resulting tumor was positive for cytokeratins 19 and 7, markers of pancreatic duct (histology not shown). In tissue culture, the 634NOD cells expressed Erc/Mesothelin (Fig. 4A), and N-ERC could be detected in the culture supernate (389.4 ± 11.7 ng/ml) (Fig. 4B). C-ERC levels were extremely low to undetectable (Fig. 4B). Taken together, the results reported here clearly indicate that the elevated N-ERC detected in the serum of transgenic rats bearing pre-malignant pancreatic lesions was derived from these lesions.

To determine whether serum levels of N-ERC correlated with tumor size, we assayed N-ERC levels in NOD-SCID mice with transplanted 634NOD cells. N-ERC was detected in the serum of these mice. Increase in the serum level of N-ERC correlated with increased with tumor size (R = 0.918, P < 0.001) (Fig. 4C). This result indicates a causal relationships between serum level of N-ERC and tumor size.

Serum N-ERC levels in rats with tumors such as bladder transitional cell tumors, liver cell tumors, lung, kidney, thyroid, mammary, prostate, and skin tumors induced by chemical carcinogens were not significantly elevated compared to their respective controls (data not shown).

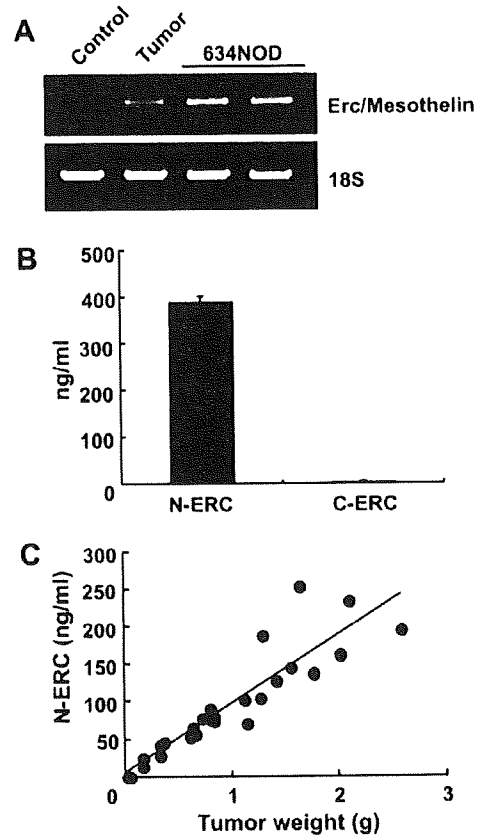

Fig. 4. The Erc/Mesothelin gene was expressed in an established pancreas ductal carcinoma cell line. (A) RT-PCR for Erc/Mesothelin in a pancreas carcinoma cell line. Control: pancreas from empty vector treated Hras250 rats (pooled sample from five animals). Tumor: pancreas carcinomas from AxCANCre injected Hras250 rats (pooled sample from five animals). 634NOD: pancreas carcinoma cell line (established from a pancreas tumor from an AxCANCre injected Hras250 rat). (B) Levels of N- and C-terminal derived Erc/Mesothelin (N-ERC and C-ERC, respectively) protein in the culture medium from a pancreas carcinoma cell line. The precursor protein is cleaved by a furin-like protease: a 31 kDa NH_2-terminal half (N-ERC) is released into the extracellular space, leaving the 40 kDa COOH-terminal half (Mesothelin) attached to the cell surface by a GPI-anchor. (C) Serum level of N-ERC in 634NOD transplanted NOD-SCID mice. The serum level of N-ERC correlated with increased tumor weight (R = 0.918, P < 0.001).

Discussion

For the purpose of developing methods to detect early cancer lesions, preferably at a preclinical stage, use of an appropriate animal model is advantageous because of the experimental availability of early lesions. To the best of our knowledge, available serum markers for cancer in animal models are limited to prostate cancer [22]. Antibodies for pancreas tumor associated human serum markers CA19-9, Dupan-2 and SPan-1 recognize carbohydrate chains, such as Sialyl Le^a, Sialyl Le^c. In this study, we found that serum levels of CA19-9, Dupan-2, and SPan-1 were below detectable levels in pancreas tumor-bearing rats regardless of stage. Cross-reactivity of these antibodies for human tumor carbohydrate antigen in rodents has not been clearly demonstrated. We have established rat models of pancreas ductal carcinomas. These models use a human $Hras^{G12V}$ (Hras250) [4] or a human $Kras^{G12V}$ (Kras327) oncogene under the control of the Cre/loxP system to induce cancerous lesions. Neoplastic lesions in the *ras* Tg rats exhibited morphological and biological similarities to those observed in human pancreas lesions. Using these models, we showed that preclinical pancreas ductal neoplasms can be diagnosed by measuring Erc/Mesothelin in the serum (Fig. 3).

N-ERC is a 31 kDa protein that forms the N-terminal fragment of the full-length 71 kDa Erc/Mesothelin protein and is secreted into the blood of mesothelioma patients. The ELISA system used in this study was originally used for the detection of N-ERC in the serum of mesothelioma patients [16]. The system was also used to detect N-ERC in the serum of Eker rats [18,23,24], and it

clearly worked in this study to detect higher levels of N-ERC in the serum of pancreas tumor-bearing rats. The expression levels of TEF-1 mRNA in pancreas tumors correlated with that of Erc/Mesothelin in tumor tissue and N-ERC in the serum. Since Erc/Mesothelin mRNA was found at relatively low levels in the normal rat pancreas, increased serum levels of N-ERC appear to be specific for pancreas carcinomas in the *ras* Tg rat models.

Many human pancreas cancer cell lines express Erc/Mesothelin [12,21,25]. N-ERC was detected in the supernatants of cultured human pancreas cancer cells, and correlated with the expression levels of Erc/Mesothelin [25]. Although there was no significant difference in serum N-ERC concentrations between pancreas cancer patients and healthy control groups [25], Erc/Mesothelin is frequently expressed in ductal carcinoma, but not in normal pancreas or chronic pancreatitis [15,25–27]. Thus, Erc/Mesothelin expression can be found in both human and rat pancreas ductal adenocarcinoma.

Previous immunohistochemical studies showed that expression of Mesothelin is found in most epithelioid mesothelioma, nonmucinous carcinomas of the ovary, adenocarcinomas of the pancreas, some breast, uterus, colorectal and lung adenocarcinomas, but not in carcinomas of the prostate, kidney, liver, thyroid, or bladder in humans [13,27–29]. In line with human data, although we have not thoroughly examined all the different tumors induced by chemical carcinogens, available data indicates that increase in serum N-ERC level is relatively specific for PDA in rats.

One advantage of using rats is that their relatively large organ size facilitates surgical procedures. In this rat model, serum levels of N-ERC can be used for the identification of early neoplastic lesions, even in preclinical stages, and also for monitoring the further progression of carcinogenesis. The model may also be used to screen for candidate chemotherapeutic agents, which could be evaluated for human use. Furthermore, serum N-ERC may prove useful for the diagnosis of pre-symptomatic lesions for human mesothelioma or ovary cancer patients.

Acknowledgments

We thank Dr. T. Sugimura (National Cancer Center) for his valuable advice, Dr. T. Shirai (Nagoya City University) for his assistance with histological specimen preparation and advice for histological examination, Drs. M. Wei (Osaka City University), S. Tamano (DIMS institute of Medical Science), S. Yamashita and T. Ushijima (National Cancer Center) for rat serum provision, and Dr. J. Miyazaki (Osaka University) for the CAG promoter provision. We also thank Y. Morita, S. Ariji, K. Ohmi and Y. Terashima, training students, for their enthusiastic assistance with establishment of the transgenic rats.

This work was supported in part by the Grant-in-Aid for Scientific Research (C) from Japan Society for the Promotion of Science, the Grant-in-Aid for Cancer Research (15-2, 16-13, 17S-6, 20S-8), the Grant-in-Aid for Research on Nanotechnical Medical (H19-nano-ippan-014), the Grant-in-Aid for Research on Risk of Chemical Substances (H18-kagaku-ippan-007, H19-Kagaku-Ippan-006) from the Ministry of Health, Labour, and Welfare of Japan, and Grant-in-Aid for Food Safety Commission, Japan (051).

References

[1] H.G. Beger, B. Rau, F. Gansauge, B. Poch, K.H. Link, Treatment of pancreatic cancer: challenge of the facts, World J. Surg. 27 (2003) 1075–1084.
[2] A. Jemal, R. Siegel, E. Ward, T. Murray, J. Xu, M.J. Thun, Cancer statistics, 2007, CA Cancer J. Clin. 57 (2007) 43–66.
[3] E.P. DiMagno, H.A. Reber, M.A. Tempero, AGA technical review on the epidemiology, diagnosis, and treatment of pancreatic ductal adenocarcinoma, Am. Gastroenterol. Assoc. Gastroenterol. 117 (1999) 1464–1484.
[4] S. Ueda, K. Fukamachi, Y. Matsuoka, N. Takasuka, F. Takeshita, A. Naito, M. Iigo, D.B. Alexander, M.A. Moore, I. Saito, T. Ochiya, H. Tsuda, Ductal origin of pancreatic adenocarcinomas induced by conditional activation of a human Ha-ras oncogene in rat pancreas, Carcinogenesis 27 (2006) 2497–2510.
[5] O. Hino, E. Kobayashi, M. Nishizawa, Y. Kubo, T. Kobayashi, Y. Hirayama, S. Takai, Y. Kikuchi, H. Tsuchiya, K. Orimoto, K. Kajino, T. Takahara, H. Mitani, Renal carcinogenesis in the Eker rat, J. Cancer Res. Clin. Oncol. 121 (1995) 602–605.
[6] Y. Yamashita, M. Yokoyama, E. Kobayashi, S. Takai, O. Hino, Mapping and determination of the cDNA sequence of the Erc gene preferentially expressed in renal cell carcinoma in the Tsc2 gene mutant (Eker) rat model, Biochem. Biophys. Res. Commun. 275 (2000) 134–140.
[7] K. Chang, I. Pastan, Molecular cloning of mesothelin, a differentiation antigen present on mesothelium, mesotheliomas, and ovarian cancers, Proc. Natl. Acad. Sci. USA 93 (1996) 136–140.
[8] T. Kojima, M. Oh-eda, K. Hattori, Y. Taniguchi, M. Tamura, N. Ochi, N. Yamaguchi, Molecular cloning and expression of megakaryocyte potentiating factor cDNA, J. Biol. Chem. 270 (1995) 21984–21990.
[9] K. Chang, L.H. Pai, J.K. Batra, I. Pastan, M.C. Willingham, Characterization of the antigen (CAK1) recognized by monoclonal antibody K1 present on ovarian cancers and normal mesothelium, Cancer Res. 52 (1992) 181–186.
[10] K. Chang, I. Pastan, M.C. Willingham, Isolation and characterization of a monoclonal antibody, K1, reactive with ovarian cancers and normal mesothelium, Int. J. Cancer 50 (1992) 373–381.
[11] K. Chang, I. Pastan, Molecular cloning and expression of a cDNA encoding a protein detected by the K1 antibody from an ovarian carcinoma (OVCAR-3) cell line, Int. J. Cancer 57 (1994) 90–97.
[12] N. Yamaguchi, K. Hattori, M. Oh-eda, T. Kojima, N. Imai, N. Ochi, A novel cytokine exhibiting megakaryocyte potentiating activity from a human pancreatic tumor cell line HPC-Y5, J. Biol. Chem. 269 (1994) 805–808.
[13] N. Scholler, N. Fu, Y. Yang, Z. Ye, G.E. Goodman, K.E. Hellstrom, I. Hellstrom, Soluble member(s) of the mesothelin/megakaryocyte potentiating factor family are detectable in sera from patients with ovarian carcinoma, Proc. Natl. Acad. Sci. USA 96 (1999) 11531–11536.
[14] C.D. Hough, C.A. Sherman-Baust, E.S. Pizer, F.J. Montz, D.D. Im, N.B. Rosenshein, K.R. Cho, G.J. Riggins, P.J. Morin, Large-scale serial analysis of gene expression reveals genes differentially expressed in ovarian cancer, Cancer Res. 60 (2000) 6281–6287.
[15] P. Argani, C. Iacobuzio-Donahue, B. Ryu, C. Rosty, M. Goggins, R.E. Wilentz, S.R. Murugesan, S.D. Leach, E. Jaffee, C.J. Yeo, J.L. Cameron, S.E. Kern, R.H. Hruban, Mesothelin is overexpressed in the vast majority of ductal adenocarcinomas of the pancreas: identification of a new pancreatic cancer marker by serial analysis of gene expression (SAGE), Clin. Cancer Res. 7 (2001) 3862–3868.
[16] K. Shiomi, H. Miyamoto, T. Segawa, Y. Hagiwara, A. Ota, M. Maeda, K. Takahashi, K. Masuda, Y. Sakao, O. Hino, Novel ELISA system for detection of N-ERC/mesothelin in the sera of mesothelioma patients, Cancer Sci. 97 (2006) 928–932.
[17] K. Shiomi, Y. Hagiwara, K. Sonoue, T. Segawa, K. Miyashita, M. Maeda, H. Izumi, K. Masuda, M. Hirabayashi, T. Moroboshi, T. Yoshiyama, A. Ishida, Y. Natori, A. Inoue, M. Kobayashi, Y. Sakao, H. Miyamoto, K. Takahashi, O. Hino, Sensitive and specific new enzyme-linked immunosorbent assay for N-ERC/Mesothelin increases its potential as a useful serum tumor marker for mesothelioma, Clin. Cancer Res. 14 (2008) 1431–1437.
[18] M. Nakaishi, K. Kajino, M. Ikesue, Y. Hagiwara, M. Kuwahara, H. Mitani, Y. Horikoshi-Sakuraba, T. Segawa, S. Kon, M. Maeda, T. Wang, M. Abe, M. Yokoyama, O. Hino, Establishment of the enzyme-linked immunosorbent assay system to detect the amino terminal secretory form of rat Erc/Mesothelin, Cancer Sci. 98 (2007) 659–664.
[19] Y. Hagiwara, Y. Hamada, M. Kuwahara, M. Maeda, T. Segawa, K. Ishikawa, O. Hino, Establishment of a novel specific ELISA system for rat N- and C-ERC/mesothelin. Rat ERC/mesothelin in the body fluids of mice bearing mesothelioma, Cancer Sci. 99 (2008) 666–670.
[20] M. Asamoto, T. Ochiya, H. Toriyama-Baba, T. Ota, T. Sekiya, M. Terada, H. Tsuda, Transgenic rats carrying human c-Ha-ras proto-oncogenes are highly susceptible to *N*-methyl-*N*-nitrosourea mammary carcinogenesis, Carcinogenesis 21 (2000) 243–249.
[21] T. Hucl, J.R. Brody, E. Gallmeier, C.A. Iacobuzio-Donahue, I.K. Farrance, S.E. Kern, High cancer-specific expression of mesothelin (MSLN) is attributable to an upstream enhancer containing a transcription enhancer factor dependent MCAT motif, Cancer Res. 67 (2007) 9055–9065.
[22] I.V. Huizen, G. Wu, M. Moussa, J.L. Chin, A. Fenster, J.C. Lacefield, H. Sakai, N.M. Greenberg, J.W. Xuan, Establishment of a serum tumor marker for preclinical trials of mouse prostate cancer models, Clin. Cancer Res. 11 (2005) 7911–7919.
[23] O. Hino, Multistep renal carcinogenesis in the Eker (Tsc 2 gene mutant) rat model, Curr. Mol. Med. 4 (2004) 807–811.
[24] M. Maeda, O. Hino, Molecular tumor markers for asbestos-related mesothelioma: serum diagnostic markers, Pathol. Int. 56 (2006) 649–654.
[25] K. Inami, K. Kajino, M. Abe, Y. Hagiwara, M. Maeda, M. Suyama, S. Watanabe, O. Hino, Secretion of N-ERC/mesothelin and expression of C-ERC/mesothelin in human pancreatic ductal carcinoma, Oncol. Rep. 20 (2008) 1375–1380.
[26] R. Hassan, Z.G. Laszik, M. Lerner, M. Raffeld, R. Postier, D. Brackett, Mesothelin is overexpressed in pancreaticobiliary adenocarcinomas but not in normal pancreas and chronic pancreatitis, Am. J. Clin. Pathol. 124 (2005) 838–845.
[27] N.G. Ordonez, Application of mesothelin immunostaining in tumor diagnosis, Am. J. Surg. Pathol. 27 (2003) 1418–1428.
[28] N.G. Ordonez, Value of mesothelin immunostaining in the diagnosis of mesothelioma, Mod. Pathol. 16 (2003) 192–197.
[29] H.F. Frierson Jr., C.A. Moskaluk, S.M. Powell, H. Zhang, L.A. Cerilli, M.H. Stoler, H. Cathro, G.M. Hampton, Large-scale molecular and tissue microarray analysis of mesothelin expression in common human carcinomas, Hum. Pathol. 34 (2003) 605–609.